Atmos. Chem. Phys. Discuss., 11, 9249–9312, 2011
www.atmos-chem-phys-discuss.net/11/9249/2011/
doi:10.5194/acpd-11-9249-2011

Atmospheric Chemistry and Physics Discussions

In situ observations of new particle formation in the tropical upper troposphere: the role of clouds and the nucleation mechanism

R. Weigel[1], S. Borrmann[1,2], J. Kazil[3,4], A. Minikin[5], A. Stohl[6], J. C. Wilson[7], J. M. Reeves[7], D. Kunkel[2], M. de Reus[1], W. Frey[2], E. R. Lovejoy[3], C. M. Volk[8], S. Viciani[9], F. D'Amato[9], F. Cairo[10], H. Schlager[5], K. S. Law[11], G. N. Shur[12], G. V. Belyaev[13], and J. Curtius[1,*]

[1]Institut für Physik der Atmosphäre, Johannes Gutenberg-Universität, Mainz, Germany
[2]Abteilung Partikelchemie, Max-Planck-Institut für Chemie, Mainz, Germany
[3]Cooperative Institute for Research in Environmental Sciences (CIRES), University of Colorado, Boulder, Colorado, USA
[4]NOAA Earth System Research Laboratory, Boulder, Colorado, USA
[5]Institut für Physik der Atmosphäre, Deutsches Zentrum für Luft- und Raumfahrt (DLR), Oberpfaffenhofen, Germany
[6]Norwegian Institute for Air Research (NILU), Kjeller, Norway
[7]Department of Engineering, University of Denver, Denver, Colorado, USA

[8] Department of Physics, University of Wuppertal, Germany
[9] Istituto Nazionale di Ottica, Consiglio Nazionale delle Ricerche, Firenze, Italy
[10] Istituto di Scienze dell'Atmosfera e del Clima ISAC-CNR, Consiglio Nazionale delle Ricerche, Italy
[11] UPMC Univ. Paris 06; Université Versailles St-Quentin; CNRS/INSU, UMR 8190, LATMOS-IPSL, Paris, France
[12] Central Aerological Observatory, Dolgoprudny, Moskow Region, Russia
[13] MDB-Myasishchev Design Bureau, Zhukovsky-5, Moscow Region, Russia
[*] now at: Institut für Atmosphäre und Umwelt, Experimentelle Atmosphärenforschung, Goethe-Universität Frankfurt/Main, Germany

Received: 8 March 2011 – Accepted: 15 March 2011 – Published: 21 March 2011

Correspondence to: R. Weigel (weigelr@uni-mainz.de)

Published by Copernicus Publications on behalf of the European Geosciences Union.

ACPD
11, 9249–9312, 2011

Abstract

New particle formation which generates ultrafine aerosol was observed in the continental tropical Upper Troposphere (UT) and Tropical Tropopause Layer (TTL), particularly at the bottom of the TTL, by in situ airborne measurements over South America (January–March, 2005) and West Africa (August, 2006). Measurements with a set of condensation particle counters with different d_{p50} (50% detection efficiency cut-off particle diameter) were conducted in the altitude range of 12.0–20.5 km on board the high altitude research aircraft M-55 "Geophysica" and at up to 11.5 km altitude on board the research aircraft DLR Falcon-20. Concentrations of ultrafine particles in the size range of 6 to 15 nm were derived from these measurements and several events of new particle formation (NPF) were identified. For two flight segments (24 February 2005 and 7 August 2006, at 12.5 km altitude) when recent lifting had influenced the probed air mass, the concentration of ultrafine particles reached up to 16 000 particles cm^{-3} (ambient concentration). A sensitivity study by using an aerosol model which includes neutral and ion induced nucleation processes revealed predicted concentrations of ultrafine particles in reasonable agreement with the in situ observations. NPF over South America was observed in cloud free air, above thin cirrus, while over West Africa, in the outflow of a Mesoscale Convective System (MCS), newly formed particles in the range of several hundred per cm^3 were found to coexist with ice cloud particles as long as the concentration of cloud particles ($d_p > 2\,\mu m$) remained below 2 cm^{-3}. The occurrence of NPF within the upper troposphere and the TTL was generally confined within an altitude band extending from 340 K to 380 K potential temperature, of particular strength between 350 K and 370 K. By means of a heated aerosol inlet line (at 250 °C) measurements of particle volatility were performed which show that within the TTL over South America and West Africa, on average 10–25% of the particles contained non-volatile cores. In background UT/TTL conditions the fractions of non-volatile particles typically ranged up to 50%. Our measurements provide further evidence for the hypothesis that the tropical UT and the TTL are aerosol source regions supplying

ACPD
11, 9249–9312, 2011

freshly nucleated particles which, if lifted, may contribute to maintain the stratospheric background aerosol. These particles can become important for cloud formation in the tropical upper troposphere, if they further grow such that they can act as cloud condensation nuclei.

1 Introduction

Increasing evidence suggests that the upper tropical troposphere is one of the most important source regions for the global stratospheric aerosol and the Junge background layer (Brock et al., 1995; Borrmann et al., 2010). However, an evaluation of the different mechanisms forming new particles by Lucas and Akimoto (2006) revealed that qualitatively, due to the large uncertainties of parameterizations, NPF is inadequately considered in global models. Ultrafine aerosol particles nucleate within the UT (Upper Troposphere) and in the TTL (Tropical Transition Layer) altitude region from gaseous precursors, and grow to stable and detectable sizes (e.g. >3 nm in diameter). This process is commonly referred to as "new particle formation" (NPF), or earlier as "nucleation event", and is detected in situ by condensation particle counters (CPC). Once formed, the particles are subject to microphysical processes (like coagulation, growth by condensation of water vapor and other gases, evaporation, scavenging, sedimentation) and can, in the tropics, be transported upward into the stratosphere. Strong new particle formation in burst-like events occurs in the UT/TTL as a consequence of the oxidation of, e.g., SO_2 which is emitted by volcanoes, at the ocean surface, or by anthropogenic sources and transported vertically into the UT by deep convection (Thornton et al., 1997) and occasionally by direct injections of SO_2 from explosive volcanic eruptions (Wilson et al., 1993) into the stratosphere. The aerosol population and its size distribution in the lower stratosphere develop by condensation of sulfuric acid and water vapor from the gas phase, by coagulation processes (Hamill et al., 1997), and removal processes like sedimentation. In situ observations of the number concentration of ultrafine aerosol in the tropical upper troposphere are rare, and ground-based as well as

ACPD
11, 9249–9312, 2011

satellite-borne remote-sensing is hampered by the small sizes of such particles. Brock et al. (1995) identified remnants of recent NPF in tropical upper tropospheric cloud-free air by aircraft borne in situ detection of high total aerosol number concentrations and concurrent high levels of particle volatility. Lee et al. (2003) reported encounters with recent NPF events in 20% of their samples (i.e. flight segments) from altitudes between 7 and 20 km in the tropics. The average number concentration was 1100 particles cm^{-3} in the particle size range between 4 and 9 nm. One conclusion from this study was that ion-induced NPF, the homogeneous nucleation process driven by the abundant presence of ionized air molecules, might have been responsible for some of these NPF events. Lee et al. (2004) also found nucleation events inside subtropical and tropical cirrus clouds between 7 and 16 km over Florida. Evidence for recent NPF was found in 72% of their in-cloud samples and in 56% of the samples outside of clouds. According to a very recent study by Frey et al. (2011) such new particle formation events seem to commonly occur inside the anvils and cirrus decks of West African MCS cloud systems. Twohy et al. (2002) suggested that mid-latitude MCS play a particular role as a source of new particles in the upper troposphere based on in situ detection of elevated total aerosol number concentrations ($d_p > 25$ nm) with increased levels of particle volatility. Thus, the question arises to what extent MCS related cirrus decks themselves are a significant source of ultrafine particles at the TTL bottom. Most other in situ observations of new particle formation in the free troposphere originate from altitudes below 12 km (Clarke et al., 1998, 1999; Clarke and Kapustin, 2002; Weber et al., 1995, 1999; Krejci et al., 2003; Crumeyrolle et al., 2010) and aloft in the upper troposphere (Hermann et al., 2003; Minikin et al., 2003). This is below the TTL and at altitudes where various types of clouds likely scavenge freshly nucleated particles before they can reach the stratosphere. Particles found in the (tropical) upper free troposphere generally consist of sulfuric acid, water, and organic compounds with some fraction of non-volatile materials (e.g. Murphy et al., 1998; Curtius et al., 2001b; Heald et al., 2005; Murphy et al., 2006; Froyd et al., 2010; Borrmann et al., 2010). The non-volatile components may be soot, mineral dust, biomass-burning residues, meteoric ablation

ACPD
11, 9249–9312, 2011

condensates, inorganic salts, and others. According to measurements from the tropics in West Africa, Northern Australia, and Brazil (Borrmann et al., 2010) up to 50% of the submicron aerosol particles between 370 K and 440 K potential temperature (Θ) levels contain non-volatile residuals with the implication that these are not pure H_2SO_4-H_2O solution droplets. A major source for pure H_2SO_4-H_2O solution droplets in the UT/TTL is homogeneous nucleation following the oxidation of precursor gases like OCS, CS_2, and SO_2 (Thomason and Peter, 2006; Wilson et al., 2008) from volcanic activity, sea surface emissions or of anthropogenic origin, e.g. by gaseous pollution material which undergoes long range transport aloft into the TTL (Law et al., 2010). Recent studies (e.g. Metzger et al., 2010; Kerminen et al., 2010) have argued that in addition to sulfuric acid also organic molecules are likely to be involved not only in particle growth but also in the initial steps of particle nucleation. However, these studies were focused on conditions in the lower troposphere.

Sulfur dioxide (SO_2), which is released from the ground appears in the boundary layer in mixing ratios ranging from 20 pptv to more than 1 ppbv. In urban, highly polluted environments, SO_2 mixing ratios of up to several hundred ppbv can be reached (Seinfeld and Pandis, 2006). Boundary layer SO_2 can be transported to the UT quickly when ingested by a cumulonimbus cloud (Cb). Although some of the SO_2 will be scavenged and dissolved by cloud hydrometeors, a major fraction does reach the Cb anvil or the outflow region unprocessed according to model calculations (Barth et al., 2001). Particularly in the tropics, where the Cb outflow occurs in the UT or lower TTL, elevated ultra-violet radiation levels cause rapid production of OH radicals and efficient oxidation of SO_2 to H_2SO_4. This mechanism in combination with low temperatures may lead to observation of NPF near or inside high altitude tropical ice clouds (Lee et al., 2004).

With respect to the physico-chemical processes underlying NPF from the gas phase several alternative mechanisms have been under consideration. These are: (1) binary homogeneous nucleation of sulfuric acid and water (Weber et al., 1999), (2) ternary nucleation of sulfuric acid, water, and a third substance like ammonia (Merikanto et al., 2007) or an organic compound (Zhang et al., 2004; Ekman et al., 2008; Metzger et al.,

ACPD
11, 9249–9312, 2011

2010; Kulmala et al., 2006; Kerminen et al., 2010), and (3) ion-induced nucleation of H_2SO_4-H_2O clusters (Curtius et al., 2006; Kazil and Lovejoy, 2004; Kazil et al., 2006; Lee et al., 2003; Yu and Turco, 2001, Kazil et al., 2007). Isobaric mixing of two subsaturated air masses can result in supersaturation (e.g. with respect to H_2SO_4) and enhance the NPF processes considerably (Khosrawi and Konopka, 2003).

Ion-induced nucleation has been suggested to be a key mechanism for NPF, initialized by ions which are formed by cosmic rays in the atmosphere. Ion production in the atmosphere is caused by lightning discharge as well. This process might have particular impact in the tropical atmosphere where convection frequently drives the formation of thunderstorm cells. Nevertheless, the expected lifetime of lightning generated ions in a thunderstorm cloud might be short, due to elevated surface area concentrations, as provided by hydrometeors, onto which these ions can rapidly attach and thus are neutralized. In case these ions live sufficiently long they could contribute to charged (ion-induced) NPF. Indications are provided by Huntrieser et al. (2002) that NPF might be strongly connected to lightning-induced physico-chemical mechanisms in mid-latitude thunderstorms. They found elevated number concentrations of presumably newly formed condensation nuclei (>30 000 particles per cm^3) in the thunderstorm outflow concurrently with increased lighting-induced NO_x (=NO and NO_2) concentrations over Europe.

While condensation of supersaturated gases preferably occurs onto pre-existing surfaces, e.g. cloud elements or surface-emitted aerosol particles, it also contributes to the growth of neutral and charged molecular clusters that have formed from the gas phase. The growth of these molecular clusters is, however, generally hindered by a nucleation barrier, as it requires extending their surface area against the associated surface tension, which consumes energy (Curtius, 2006). As a consequence, even when the gaseous substances are supersaturated, and in absence of pre-existing aerosol, this barrier often prevents NPF in the atmosphere to occur in significant amounts. Ions potentially act as nucleation cores for the attachment of supersaturated gas phase molecules by reducing the height of the nucleation barrier due to the

ACPD
11, 9249–9312, 2011

stabilizing electrostatic interaction between the ionic charge and the ligand molecules (Lovejoy et al., 2004; Curtius et al., 2006). Thermodynamically, the ion-induced NPF process is more favorable than neutral homogeneous nucleation, but the maximum amount of particles produced via the ion pathway is limited by the ion production rate. Large ions have been detected by Eichkorn et al. (2002) in the upper troposphere. First aircraft measurements with an air ion spectrometer in mid-latitudes were performed by Mirme et al. (2010) who found a minor importance of ion-induced nucleation from their measurements in the free troposphere. Whether this spatially limited data set is representative for other conditions, regions and altitudes remains to be shown.The question whether or not ion-induced processes contribute to the overall NPF is by far not unambiguously answered. The processes leading to NPF, the dependency of the one or the other process on the given preconditions, are not yet fully understood.

One purpose of this study is to present the data from in situ measurements in the tropical UT/TTL over South America and West Africa performed during the TROCCINOX and SCOUT-AMMA campaigns, respectively, and to discuss the occurrence of NPF within the upper troposphere and TTL region. Observations from two flights are discussed in detail, demonstrating several cases of recent new particle formation of variable strength. Sensitivity studies with an aerosol nucleation model are presented for investigating the strength of NPF under different environmental conditions, and to investigate whether observed concentrations of newly formed particles can be reproduced by the model. The role of SO_2 and pre-existing aerosol for the nucleation process in the UT/TTL is discussed, as is the presence of newly formed particles in ice clouds.

ACPD
11, 9249–9312, 2011

2 Field campaign data base and instrumentation

2.1 Campaign locations and research aircraft

In order to obtain in situ field measurements within the TTL and the tropical UT the Russian high altitude research aircraft M-55 "Geophysica" operated at altitudes up to 20.5 km. The DLR Falcon-20 covered the altitude range from the ground to the tropical middle troposphere reaching 11.5 km. Both aircraft were deployed:

1. during the TROCCINOX-2 field campaign ("Tropical Convection, Cirrus, and Nitrogen Oxides Experiment"; January–March 2005, from Araçatuba, Brazil, at 21.1° S, 50.4° W; see Schumann, 2005; Schumann and Huntrieser, 2007) and
2. during SCOUT-AMMA (August 2006, from Ouagadougou, Burkina Faso, at 12.4° S, 1.5° W; see Cairo et al., 2010).

Both field missions aimed at investigations, beside others, concerning the influence of tropical convection on the UT/TTL composition, and its impact on the tropical stratosphere and the subtropical lowermost stratosphere (LS). During the TROCCINOX measurement period the local meteorology was predominantly influenced by the quasi-stationary pressure systems, the "Bolivian high". Frequent MCS formation over southeast America (partly covering Argentina, Brazil, Paraguay and Uruguay) occurred and influenced the probed air masses as well as isolated thunder storms (Konopka et al., 2007). These authors analyzed the air mass transport and mixing across the TTL over Brazil. The studies of Schiller et al. (2009) described at the transport and transformation of H_2O in the TTL and the impact on the stratospheric water budget. The air masses in the TTL over West Africa, during the SCOUT-AMMA mission, were strongly influenced by the Tropical Easterly Jet (TEJ) such that the air mass transport towards the Sahelian TTL predominantly origins from the Asian UT/LS, driven by the South Asian monsoon (Cairo et al., 2010). Fierli et al. (2011) provides indications for local convection, formed in the Sahelian region extending from Sudan to West Africa. This

ACPD
11, 9249–9312, 2011

local convection may have been superimposed on a mainly zonal air mass transport that prevailed throughout the SCOUT-AMMA mission with direct impact on the composition in the tropical UT (Fierli et al., 2011). More studies on the air masses which impact particularly the chemical composition of the gaseous and aerosol constituents in the West African TTL during SCOUT-AMMA are provided by Law et al. (2010).

The data obtained from measurements aboard the M-55 "Geophysica" which are included in the analyses of this study, cover 5 local and 4 transfer flights from TROCCINOX, as well as 5 local flights from SCOUT-AMMA. From the CPC measurements aboard the DLR Falcon-20 research aircraft data of 11 local flights and 4 transfer flights from TROCCINOX as well as 8 local and 2 transfer flights from SCOUT-AMMA are analyzed. More information on the overall results from the two missions is available in the Special Issues of *Atmospheric Chemistry and Physics:* TROCCINOX (http://www.atmos-chem-phys.net/special_issue82.html), and SCOUT-AMMA (http://www.atmos-chem-phys.net/special-issue125.html). Details on the aircraft, the instrumentation, and the campaign deployments can be obtained for TROCCINOX from "http://www.pa.op.dlr.de/troccinox/" and for SCOUT-AMMA from "http://amma.igf.fuw.edu.pl".

2.2 Instrumentation for submicron aerosol measurements

Two COPAS (COndensation PArticle counting Systems) were operated as dual-channel condensation particle counters (CPCs) at altitudes between 12.0 and 20.5 km on board the M-55 "Geophysica". The COPAS performance has been characterized by extensive laboratory and airborne experiments (Curtius et al., 2005; Weigel et al., 2009). The set of CPCs installed on board the DLR Falcon-20 aircraft for measurements from ground level to 11.5 km altitude is described by Minikin et al. (2003), Fiebig et al. (2005), and Weinzierl et al. (2009).

The smallest detectable particle size of two COPAS channels were adjusted to $d_{p50} = 6$ and 15 nm (at 150 hPa operating pressure), where d_{p50} denotes the size diameter at which particles are detected with 50% efficiency. Accordingly, the particle

ACPD
11, 9249–9312, 2011

number concentrations resulting from COPAS measurements are denoted as N_6 (for submicron particles with $d_p > 6$ nm) and N_{15} ($d_p > 15$ nm). These lower detection limits, as well as their maximum asymptotic counting efficiencies, were found to depend on the operating pressure (Hermann et al., 2005) which was accounted for in our data set according to Weigel et al. (2009). Both, the third and fourth COPAS channel were operated with a d_{p50} of 10 nm. One of these channels was equipped with an aerosol pre-heater (of 250 °C) to determine the non-volatile aerosol fraction N_{nv} (Curtius et al., 2005; Borrmann et al., 2010). The working fluid for all COPAS channels was FC-43, (perfluoro-tributylamine), because of its advantageous particle activation behavior at pressures below 200 hPa (Brock et al., 2000; Hermann et al., 2005).

Similar to the Geophysica CPCs, a CPC system on board the DLR Falcon-20 was operated at settings with $d_{p50} = 4$ nm, $d_{p50} = 10$ nm and $d_{p50} = 13$ nm (Minikin et al., 2003). Another CPC on board the DLR Falcon-20 was measuring the concentration of non-volatile particles N_{nv} by heating the sampled ambient air to 250 °C in a setup very similar to that on the M-55 "Geophysica". The difference in the count results between two channels measuring with different d_{p50} provides in general the concentration of ultrafine particles N_{uf} which represents the number density of particles at sizes between about 4 and 10 nm (or 13 nm) for the CPCs on the DLR Falcon-20 during SCOUT-AMMA (TROCCINOX), and about 6 to 15 nm for the COPAS measurements. All particle concentration data in this paper are presented as number of particles per cm^3 of air at ambient pressure and temperature. The measurements occurred at a rate of 1 Hz and are provided as 15-s running averages.

Due to payload limitations on the M-55 "Geophysica" we were not always able to operate all four COPAS channels which are pairwise integrated in two separate instrument boxes. In particular, no volatility measurements are available for the flights of 24 February 2005, and 7 August 2006.

Results from measurements in the tropical UT/TTL region near Costa Rica are also included from the University of Denver instrument NMASS (Nuclei Mode Aerosol Spectrometer; Brock et al., 2000). The NMASS consists of five continuous-flow

ACPD
11, 9249–9312, 2011

condensation particle counters (CPCs) operated in parallel at a constant system pressure of 60 hPa. The NMASS automation controls the CPC saturator-condenser temperature such that the NMASS CPCs 1 to 5 measure particle number concentrations with d_{p50} of 5.3 nm, 8.4 nm, 15 nm, 30 nm and 53 nm respectively. The NMASS was flown on the NASA WB-57F in a series of missions (Pre-AVE – Pre Aura Validation Experiment, AVE_0506 – Aura Validation Experiment, CR-AVE – Costa Rica Aura Validation Experiment and TC4 – Tropical Composition, Cloud and Climate Coupling) aiming at aerosol measurements in the UT/TTL in the tropics of the Americas. The flights originated from Houston, (USA) and San Jose (Costa Rica). The NMASS data used were measured south of 23° N and between 95.1° and 78.2° W (around Central America) in January and February of 2004, in June 2005, in January and February of 2006 and during August 2007. Data which were acquired in recognized plumes from aircraft were excluded.

2.3 Instrumentation for cloud measurements

Some of the NPF encountered by the M-55 "Geophysica" occurred inside clouds. For their characterization the cloud particle size distributions were measured by a Forward Scattering Spectrometer Probe (modified FSSP-100, Dye and Baumgardner, 1984; De Reus et al., 2009) during TROCCINOX. During SCOUT-AMMA a Cloud Imaging Probe (CIP) was deployed besides the FSSP-100. The FSSP-100 measurement range covers particle size diameters from 2.5 µm to 30 µm while the CIP detects and images particles with sizes from 25 µm to 1.6 mm (De Reus et al., 2009; Frey et al., 2011). The methods applied for the data reduction of the FSSP-100 and CIP measurements and the corresponding error analyses are described in De Reus et al. (2009) and Frey et al. (2011).

In addition, the Multiwavelength Aerosol Scatterometer (MAS; Buontempo et al., 2006; Cairo et al., 2011) was implemented on the M-55 "Geophysica" to detect the presence of clouds during flight. Responding to the presence of optically active particles with sizes above 0.2 µm the MAS also provides measurements of aerosol

ACPD
11, 9249–9312, 2011

backscatter and depolarization (at 532 nm and 1064 nm wavelengths) in the immediate vicinity of the aircraft with 5 s time resolution and 5% accuracy.

2.4 Instrumentation for gas phase tracer species and flight parameters

Carbon dioxide (CO_2) measurements with 5 s time resolution were performed on board the M-55 "Geophysica" with the High Altitude Gas AnalyzeR (HAGAR, Riediger, 2000; Homan et al., 2010), which is a two-channel in situ gas chromatograph. Carbon monoxide (CO) is measured by the COLD (Cryogenically Operated Laser Diode; Viciani et al., 2008) instrument with 0.25 Hz sampling rate, 1% precision, and with an accuracy of 6–9%. The measurement of the ambient temperature was performed with the Thermo Dynamic Complex (TDC) probe with an accuracy of 0.5 K (Shur et al., 2007). Further relevant flight parameters are provided by the M-55 "Geophysica" navigational system Unit for Connection with the Scientific Equipment (UCSE, Sokolov and Lepuchov, 1998).

3 Modeling tools for the case studies of new particle formation events

One goal of the case studies presented below is to provide model estimates of new particle formation rates and corresponding concentrations based on microphysical processes for direct comparison with the in situ measured number densities N_{uf}. Therefore, MAIA (Model of Aerosols and Ions in the Atmosphere) developed by Lovejoy et al. (2004) and Kazil et al. (2007) was applied. As input parameters for MAIA in situ data and estimates of SO_2 mixing ratios derived from FLEXPART/FLEXTRA model results were used.

3.1 FLEXPART model for emission sensitivity studies

Oxidation of SO_2 to H_2SO_4 vapor with subsequent nucleation is considered as the process driving NPF events which are described in the presented case studies.

ACPD
11, 9249–9312, 2011

Consequently, it is important to quantify the amount of SO_2 which was available for oxidation in an air parcel along its trajectory until it was intercepted and sampled by the research aircraft. Estimates of anthropogenic SO_2 emission source strengths from the EDGAR global inventory were used and the transport of air masses was simulated by means of the Lagrangian particle dispersion model FLEXPART (Stohl et al., 1998, 2005). So-called retro-plumes (see Stohl et al., 2003) were initialized at short time intervals along the flight tracks of the M-55 "Geophysica". The simulations are based on operational data from ECMWF with a horizontal resolution of 1° globally and 0.5° in the measurement area, and a time resolution of 3 h. Generally 60 vertical levels were considered with additional 31 for the SCOUT-AMMA flights. Each simulation consists of the trajectories of 40 000 air parcels that are released in the volume of air sampled by the aircraft instrumentation and tracked for 20 days backward in time. Stochastic fluctuations, obtained by solving Langevin equations, are superimposed on the grid-scale winds to represent transport by turbulent eddies (Stohl et al., 2005). A convection scheme (Emanuel and Živković-Rothman, 1999) is used to represent convective transport (Forster et al., 2007). This scheme does not resolve individual subgrid-scale convective cells but represents the overall effect of convection in grid cells where convection is diagnosed by redistributing particles stochastically according to the convective mass fluxes determined by the Emanuel and Živković-Rothman (1999) scheme.

The backward simulations yield an emission sensitivity (Stohl et al., 2005, 2006) which is proportional to the residence times of the air parcels in a particular 3-D grid cell. The value of this emission sensitivity is a measure for the simulated mixing ratio in the receptor volume that a source of unit strength in the respective grid cell would produce, disregarding loss processes. The emission sensitivity can be used to display the transport history. By multiplying the emission sensitivity near the ground with an emission flux (here, anthropogenic SO_2 emissions from the EDGAR global inventory), maps of source contributions are obtained, which can be used to identify pollution sources. Spatial integration of the source contributions yields the simulated mixing

ACPD
11, 9249–9312, 2011

ratio of a passive tracer (here, of all anthropogenic SO_2 emissions accumulated over the past 20 days) along the flight track.

3.2 FLEXTRA model for trajectory analyses

The box model used to describe aerosol nucleation runs on single "representative" trajectories and requires meteorological data along these trajectories as input. To produce back trajectories of single air masses from along the flight track, we used the trajectory model FLEXTRA (Stohl et al., 1995, 2001), driven with the same meteorological input data as FLEXPART. These calculations are based only on the grid-scale ECMWF winds and represent convection only to the extent resolved by the ECMWF data. Nevertheless, trajectories with strong ascent were found for the convectively influenced flight segments of interest. We furthermore subjectively selected those trajectories with the strongest ascent for the MAIA calculations, assuming that they best represent the overall lifting of NPF precursors into the UT/TTL, thus compensating for the fact that single trajectories cannot represent sub-grid-scale convective lifting. There was good qualitative agreement between the selected single strongly ascending trajectories calculated by the FLEXTRA and the FLEXPART model results for the corresponding flight segments, both indicating transport from the boundary layer in the same region.

3.3 Physico-chemical model MAIA for neutral and ion-induced aerosol nucleation

MAIA (Lovejoy et al., 2004; Kazil et al., 2007) describes oxidation of SO_2 to gaseous H_2SO_4, nucleation of neutral and charged sulfuric acid-water aerosol particles, aerosol condensational growth, and coagulation of the aerosol particles among each other and onto pre-existing particles. Nucleation is implemented in the model based on laboratory thermo-chemical data (Curtius et al., 2001a; Lovejoy and Curtius 2001; Froyd and Lovejoy 2003a and b; Hanson and Lovejoy, 2006) for H_2SO_4 uptake and loss by neutral and charged clusters with up to 2 and 5 sulfuric acid molecules, respectively. MAIA uses laboratory thermo-chemical data (Gibbs' free energy of formation) to

ACPD
11, 9249–9312, 2011

describe the stability (decay probability) of the smallest neutral and charged clusters, which is essential for the reliable description of the nucleation process. Gibbs' free energy also gives the temperature dependence of the cluster stability (decay probability). Hence MAIA describes neutral and charged nucleation down to the very low temperatures occurring in the upper troposphere and lower stratosphere. The thermochemical data for H_2SO_4-H_2O uptake and loss by large H_2SO_4-H_2O aerosol particles ($\gg$5 sulfuric acid molecules) originate from the liquid drop model and H_2SO_4 and H_2O vapor pressures over bulk solutions as calculated with a computer code (provided by S. L. Clegg, personal communication, 2007) which adopts experimental data from Giauque et al. (1960) and Clegg et al. (1994). The thermo-chemical data for intermediate sized particles are a smooth interpolation (see Kazil et al., 2007) of the data for the small (neutral clusters with 2 and charged clusters with 5 sulfuric acid molecules) and large particles ($\gg$2 or 5 sulfuric acid molecules). The rate coefficients for sulfuric acid uptake and loss by the aerosol particles, for the coagulation of the aerosol particles, and for the recombination of the negatively charged aerosol with cations are calculated with the Fuchs formula for Brownian coagulation (Fuchs, 1964) and averaged over the equilibrium H_2O content probability distribution of the aerosol. This simplification holds well in the troposphere up to UT/LS altitudes, where water is more abundant by orders of magnitude than sulfuric acid, so that the aerosol particles have ample time to equilibrate with respect to water uptake or loss before colliding with a H_2SO_4 molecule. The system of differential equations for the aerosol concentrations is integrated with the VODE (Variable-coefficient Ordinary Differential Equation) solver (Brown et al., 1989).

In summary, based on

1. the FLEXTRA derived estimates of temperature, relative humidity, and pressure, along a backward trajectory of air mass transport,

2. estimates of available OH (which is parameterized as a cosine of the solar zenith angle, in approximation of the diurnal cycle of OH in the troposphere – Li et al., 2005; Wang et al., 2008) and pre-existing aerosol surface area,

ACPD
11, 9249–9312, 2011

3. cosmic ray induced ion production rates, calculated by a model of energetic particle transport in the Earth's atmosphere (O'Brien, 2005), which accounts for variations in cosmic ray intensity as function of latitude and altitude,

4. initial SO_2 mixing ratios of 50 pptv or 500 pptv, representing estimated minimum and maximum levels,

MAIA calculates the number of aerosol particles produced in a NPF event (per cubic centimeter and second) as a function of daytime along particular air parcel trajectories intersecting with the M-55 "Geophysica" flight path. The diameter size range of ultrafine particles analyzed from the MAIA simulations coincides with the diameter size range of ultrafine particles measured by COPAS.

One limitation of this approach is that as both model tools MAIA and FLEXTRA do not take into account that air masses are mixed with surrounding air. Particularly during uplift or when detrainment occurs, it is very likely that in reality the lifted air mass is diluted due to mixing with background air. One has to consider that the result of FLEXPART calculations concerning the SO_2 mixing ratio represents a maximum value because SO_2 removal is ignored. Air mass mixing and resulting dilution, however, is considered by the FLEXPART model. In contrast, the single trajectories resulting from FLEXTRA and the results from MAIA simulations cannot reflect changes in SO_2 mixing ratios or aerosol surface area concentrations due to dilution or removal processes. Thus, the MAIA simulations of this work serve as a sensitivity study.

4 Results and interpretations

4.1 Overview of the new particle formation events encountered in the tropics

4.1.1 Summary of tropical submicron particle measurements

The vertical distribution of measured total submicron particle number concentration data are displayed in Fig. 1 as median profiles over all TROCCINOX (Fig. 1a) and

ACPD
11, 9249–9312, 2011

SCOUT-AMMA (Fig. 1b) flights. The data include all measurements from the M-55 "Geophysica" (number concentration N_6, for $\Theta > 350$ K, above ~11 km altitude) and the DLR Falcon-20 (N_4 for $\Theta < 350$ K). The measurements indicate a high variability in particle number concentrations at $\Theta < 310$ K (below ~2 km altitude) ranging from 1000 to 40 000 particles per cm^3. A minimum with typically less than 1000 particles per cm^3 is observed for 310 K $< \Theta <$ 330 K (~2–6 km) and a maximum in the altitude range, where NPF events were detected most frequently and with the largest number concentrations (350 K $< \Theta <$ 370 K, ~11–15 km). Generally, over West Africa and between 380 K and 420 K (~16–18 km) somewhat higher particle number concentrations were observed than over South America. Additionally, in Fig. 1c the vertical distribution of the particle number concentration from measurements with the University of Denver's NMASS is shown from measurements in the tropical UT/TTL region near Costa Rica. Displayed data show results from the first of five NMASS detection channels ($d_{p50} = 5.3$ nm). Note that in Fig. 1a and b the TROCCINOX and SCOUT-AMMA datasets are displayed separately (distinguishing measurement locations and years) while the NMASS data set (Fig. 1c) is a summarized result from measurements over 4 yr. The measurements with NMASS were performed almost at the same location in the tropics (Central America) including winter and summer seasons. However, the comparison reveals one common feature: The altitude level which is characterized by highest particles number concentrations N_6 is ranges between 350 K and 370 K, the bottom of the TTL. The lower TTL boundary is located, according to the description by Fueglistaler et al. (2009), at the 355 K level where the main convective outflow occurs. Gettelman et al. (2004) define 350 K to be the isentropic level of main deep convective outflow which is in agreement with the findings by Law et al. (2010) for the particular case of the SCOUT-AMMA mission during the 2006 monsoon season over West Africa.

4.1.2 Detection of NPF by the COPAS instrument and the DLR CPC system

N_{uf} is determined by the subtraction of aerosol number concentrations measured with two CPC channels of different d_{p50} settings, respectively. For the COPAS system this

ACPD
11, 9249–9312, 2011

is generally $N_{uf} = N_6 - N_{15}$. For the DLR CPC system N_{uf} is obtained from the difference between N_4 and N_{13} (TROCCINOX) or N_4 and N_{10} (SCOUT-AMMA). It is important to note that in background conditions the COPAS channels with $d_{p50} = 6$ nm and $d_{p50} = 15$ nm show almost equal number concentrations, within the measurement uncertainties of 15% for each channel (Weigel et al., 2009). The same is valid for the DLR CPC system within a measurement uncertainty of 10%. A definition whether or not a difference in the measurement of two CPC indicates NPF events is given with a NPF criterion. The NPF criterion for the COPAS measurements considers the measurement uncertainty of 15% for each COPAS channel. Thus, a positive difference between N_6 and N_{15}, i.e. if the N_6 concentration multiplied by 0.85 exceeds the N_{15} concentration multiplied by 1.15, indicates recent NPF observed by the COPAS instrument. According to a measurement uncertainty of 10% an NPF criterion, equivalent to the one used for the COPAS data, was applied on the measurement data from the DLR CPC system. Intentionally a conservative approach was adopted here as application of other NPF criteria, as suggested by Lee et al. (2003), on our measurements would lead to more frequent observation of NPF events with longer duration of each event.

At background conditions, without NPF, the subtraction of number concentrations that are measured by two independently operated CPCs lead to positive and negative values of N_{uf} that statistically vary around zero. Thus, only if determined N_{uf} exceeds 100 particles per cm^3 a NPF event is considered to be of significant strength.

4.1.3 Summary of NPF event data

The number concentrations of ultrafine particles N_{uf} during TROCCINOX and SCOUT-AMMA are shown as a function of potential temperature in Fig. 2a. Nucleation-mode particles often occurred at the bottom of the TTL. The cold point tropopause was located at 360–385 K during TROCCINOX and SCOUT-AMMA, but generally not above 385 K. Between 350 K and 370 K N_{uf} determined from COPAS measurements peaks to values of 4000 to 8000 particles per cm^3 with a maximum of >16 000 particles per

ACPD
11, 9249–9312, 2011

cm^3 at 375 K which was observed during the flight on 27 January 2005. The results of N_{uf} determined from measurements with the NMASS correspondingly shows the appearance of highest concentrations (>25 000 particles per cm^3) of nucleation mode particles at altitudes below 385 K. N_{uf} that was measured aboard the DLR Falcon-20, displayed in Fig. 2a, indicates numerous NPF events in the range between 340 K and 350 K exceeding the COPAS measurements at according altitude levels. This discrepancy might be caused due to the different total measurement time of both aircraft at this flight level (M-55 "Geophysica": ~4 h, DLR Falcon-20: ~31 h, over the complete mission period of TROCCINOX and SCOUT-AMMA). Between 310 K and 340 K the occurrence of NPF is clearly reduced. A further distinct layer is shown by the CPC measurement data obtained aboard the DLR Falcon-20 with elevated N_{uf} reaching up to 23 500 particles per cm^3 between 300 K and 310 K, which is well inside the boundary layer and, therefore, beyond the scope of the current study.

With COPAS the NPF events were observed in the TTL region during 4 transfer flight sections and 5 (of 9) local flights over South America as well as during each of 5 local flights over West Africa in different strength. The occurrence frequency of NPF events throughout TROCCINOX and SCOUT-AMMA and statistical parameters concerning measured N_{uf} are summarized in Table 1. During NPF events, according to the 15%-criterion (negative values of N_{uf} were set to zero), median N_{uf} were found to range between 200–900 particles per cm^3 below 350 K (Fig. 2b). Between 355 K and 360 K NPF events with median N_{uf} of more than 1000 particles per cm^3 were observed. Additionally, the variability in this altitude range is large, ranging from 250 particles per cm^3 (25-percentile) up to 4000 particles per cm^3 (75-percentile). Above 365 K until 385 K the median N_{uf} gradually decreases to 100 particles per cm^3. Above 385 K the abundance of NPF events decreases in occurrence and in strength such that the median N_{uf} generally remains below 50 particles per cm^3, thus below our limit of significance. Above 400 K the median N_{uf} do not exceed 20 particles per cm^3, apart from the exceptional case of NPF occurrence on a flight section between Recife (Brazil) and Sal (Cape Verde) on 27 February 2005 reaching N_{uf} of 100–150 particles per cm^3

ACPD
11, 9249–9312, 2011

at the 415–420 K level. It can be speculated that a NPF event at this altitudes, well within the stratosphere, might be closely connected to the stratospheric Junge aerosol layer. Moreover, this example demonstrates that elevated N_{uf} can also be observed at stratospheric altitudes. Whether or not these ultrafine particles were formed in the stratosphere would be speculative.

In Fig. 2b also the averaged N_{uf} which were determined from 68 (>350 K) and 266 (<350 K) single NPF events throughout TROCCINOX and SCOUT-AMMA are shown and color-coded according to respective duration of each event. Above 350 K, 64 NPF events were observed over periods of 15 min or less. Only 4 single NPF events with significantly larger durations of 20, 29, 31 and 43 min, respectively, were observed. Note that the M-55 "Geophysica" mean ground speed ranges at ~170(±80) m s^{-1} at altitudes above 12 km, below, according values for the DLR-Falcon 20 are ~200 (±20) m s^{-1}. Below 350 K single NPF events rarely reach durations of more than 15 min to a maximum of 25 min (2%) and exclusively between 345 K and 350 K. Generally, below 350 K, up to 76% of the NPF events were observed over less than 2 min and about 22% between 2–15 min.

On a timescale of 1–2 days after burst-like NPF events most of the ultrafine particles may either coagulate with other particles or may grow by condensation. Both would mean that particles disappear out of the ultrafine diameter size range. Since the NPF were encountered often it is conceivable that such events occur frequently in the tropical upper troposphere.

Analysis of the non-volatile particle distribution is useful to gain a better insight into the processes, e.g. of aerosol transport from elsewhere or local aerosol formation, governing the particle budget in the TTL. Therefore, the measured vertical distribution of the median number concentration for non-volatile particles N_{nv} is shown in Fig. 2c. In Fig. 2d the ratio, f, of N_{nv} and N_6 (or N_4 for the DLR Falcon-20) is displayed. The most intense events of NPF in the uppermost free troposphere and lower TTL region were encountered within a narrow altitude band, between 350 K and 360 K. In the TTL between 360 K and 380 K nucleation mode particles were frequently found in quantities

ACPD
11, 9249–9312, 2011

of several hundred up to thousands per cm^3. With respect to particle volatility, the altitudes between 340 K and 360 K (Fig. 2b and c) appear to contain the lowest amounts of non-volatile particles. A similar minimum for f has also been observed in the TTL over Northern Australia (Borrmann et al., 2010). At those levels where nucleation mode particles were detected relatively low fractions of non-volatile particles (with $f \approx 10$–20%) result. This is in agreement with the notion that freshly nucleated particles consist of solution droplets mainly containing substances which are entirely volatile at 250 °C.

At lower altitudes the variability of N_{nv} increases, partly yielding a fraction of >60% related to total particle concentrations (Borrmann et al., 2010). This demonstrates significant differences between the measurement locations in South America and West Africa, particularly at altitudes between 320 K and 340 K. However, the major difference between both missions is found at 370 K and aloft. Here N_{nv} measured during SCOUT-AMMA ($N_{nv} = 220\,cm^{-3}$) exceeds the corresponding values from TROCCINOX ($N_{nv} = 25\,cm^{-3}$) by up to one order of magnitude. This could be a result of the volcanic eruption of Soufrière Hills on Montserrat Island, Caribbean Sea, on 20 May 2006, two months before the SCOUT-AMMA mission (Borrmann et al., 2010).

4.1.4 Relevance for the TTL

The data indicate that the most intense NPF occurred at the bottom of the TTL (355 K to 360 K, see Fueglistaler et al., 2009) immediately above the main outflow region of tropical deep convection. For SCOUT-AMMA Fierli et al. (2011) showed by means of mesoscale model calculations that detrainment of convectively lifted air reached altitudes of 17 km and higher, significantly influencing the TTL over West Africa. Considering the outflow altitude range from 320 K, for shallow convection, up to 350 K, for deep convection (Law et al., 2010), it can be speculated that the minima in the particle volatility parameters N_{nv} and f just above the level of convective outflow are caused by previous scavenging of non-volatile particles during convective air mass ascent. Refining the original findings by Brock et al. (1995), we observe that the particles are mostly produced in the lowest parts of the TTL and in the UT. Fractions of these newly formed

ACPD
11, 9249–9312, 2011

particles are then amenable for being transported upward through the TTL and could reach the stratosphere (Fueglistaler et al., 2009; Borrmann et al., 2010).

The highest concentrations of ultrafine particles N_{uf} were found to cover considerable spatial range during two flights on 24 February 2005 (TROCCINOX, South America) and on 7 August 2006 (SCOUT-AMMA, West Africa). These events of NPF are discussed in detail below.

4.1.5 Case studies of three NPF events over South America and over West Africa

Three cases of NPF encounters are discussed here, one observed over South America (Case 1) and the other two over West Africa (Cases 2 and 3).

On 24 February 2005 (Case 1) the first post-mission transfer flight of the M-55 "Geophysica" was performed from Araçatuba (21° S) to Recife (8° S), Brazil. On this day the meteorological situation over the Brazil was dominated by a Bolivian high that supported the advection of air masses from the Pacific, passing over central Argentina in a counter-clockwise turn towards the Atlantic and northwards along the Brazilian East coast. A trough was northwards moving along the eastern part of Brazil connected with isolated thunderstorms over the Amazon Basin, over North East Argentina (~28° S) and over the Atlantic (~23° S).

One local flight over West Africa (10–13° N and 1.5–8° W) on 7 August 2006 (Case 2 and 3) aimed at measurements at the cloud top and in the outflow region of a dissolving intense MCS over southern Mali (Cairo et al., 2010; Fierli et al., 2011). The flight track of the M-55 "Geophysica" followed a direct approach towards the region above the MCS top and subsequent flight section allowed for measurement with increasing distance of the MCS. Finally, a new approach to the region above the same MCS occurred before the M-55 "Geophysica" turned back to the mission base. The level of main outflow of this MCS was located at the 353 K level by Fierli et al. (2011). These authors investigate the convective uplift of air masses due to this MCS and find highly variable convective ages from a few up to 48 h.

ACPD
11, 9249–9312, 2011

4.1.6 In situ measurements from South America

During the M-55 "Geophysica" flight on 24 February 2005 at ~13 km altitude large concentrations (up to 7700 particles cm^{-3}) of ultrafine particles with diameters in the size range of 6 to 15 nm were observed, indicating recent NPF (Case 1). The measured data are displayed in Fig. 3a together with other relevant variables. During Case 1, at ~14:15 UTC, the M-55 "Geophysica" encountered a cirrus cloud which is indicated by FSSP-100 measurements of increased number concentrations ($N_{>2\,\mu m}$) of particles with $d_p > 2\,\mu m$.

The large concentrations of ultrafine particles over South America are correlated with lower CO_2 concentrations indicating a different air mass history for those air masses wherein NPF occurred. It is not possible to relate the decreased CO_2 concentrations with specific sinks at ground due to the strong variability of the various sources and sinks of CO_2, e.g. diurnal cycles, distribution of vegetation, etc. The reduced CO_2 concentrations in the sampled air masses, however, are indicative for CO_2 uptake by vegetation and thus, the low CO_2 concentrations also indicate that the sampled air recently had contact with the boundary layer and most likely was carried aloft to the measurement altitudes.

4.1.7 In situ measurements from West Africa

On 7 August 2006 two pronounced NPF events with concentrations up to 4000 particles cm^{-3} were observed in the altitude range of 12 km to 14 km (see Fig. 3b, Case 2 and Case 3). The measurements of Case 2 were recorded during a period of level flight at ~13.5 km followed by a descent to 12 km and re-ascent between 13:55 and 14:16 UTC. According to measurements by MAS immediately before and after this NPF Case 2 increased backscattering and depolarization was observed which might be indicative for having passed a field of tenuous clouds.

Furthermore, NPF was observed during the descent period at 13.5 km to 12 km altitude between 15:35 and 15:40 UTC (Case 3). During Case 3 the anvil of a Mesoscale

ACPD
11, 9249–9312, 2011

Convective System (MCS) was partly crossed. The anvil contained many particles with large sizes constituting a correspondingly large surface area capable of scavenging newly formed ultrafine particles. The high values of depolarization (cf. Sect. 5.4) measured by MAS indicate the presence of aspherical particles, i.e. ice, inside the cloud.

4.2 Transport model calculations and estimation of SO_2 loadings

The FLEXPART results for the cases from South America and West Africa are shown in Fig. 4, with superimposed flight altitude (black line). The colored columns show SO_2 tracer mixing ratios simulated by FLEXPART along the flight track, with the colors indicating the time in days since emission of the SO_2 from the surface according to the EDGAR inventory (cf. Sect. 3.1). Since SO_2 was carried as a passive tracer, the mixing ratios represent the total exposure of the sampled air mass to SO_2 emissions over the last 20 days. Real SO_2 mixing ratios at the sampling locations would likely have been lower because of loss processes both within the boundary layer and during uplift to the flight altitude.

Results of FLEXPART analyses for the NPF events

The calculations with the FLEXPART model as presented in Fig. 4 indicate that the air parcels probed during the NPF events have contained potential maxima of SO_2, i.e. ~0.6 ppbv and ~1.4 ppbv for the case studies of South America and West Africa, respectively. The air masses were lifted to the measurement altitude within the last 4 to 7 days, either by convective or by slower, synoptic scale lifting. Both lifting processes are considered within the FLEXPART simulations, nevertheless, it is impossible to distinguish respective contribution to the resulting uplift. For the TROCCINOX case in the upper panel of Fig. 4 the highest source contributions of SO_2 were located along West Brazil and Peru. For the SCOUT-AMMA study in the lower panel the SO_2 source contributions were located in East Africa and East India/South-East Asia. The latter is

ACPD
11, 9249–9312, 2011

in qualitative agreement with the calculations by Law et al. (2010), who showed that ~40% of the air masses in the mid-TTL over West Africa during SCOUT-AMMA were influenced by injection of lower tropospheric air from Asia and India, while Fierli et al. (2011) concluded that over Africa regional deep convection played a role as well.

4.3 MAIA simulations of new particle formation

The purpose of the MAIA simulations is to investigate whether ion-induced and neutral aerosol formation from H_2SO_4 and H_2O suffices to explain the measured concentrations of ultrafine particles ($N_{uf} = N_6 - N_{15}$). The MAIA simulations (cf. Sect. 3.3; Lovejoy et al., 2004; Kazil and Lovejoy, 2007) are based on selected individual air mass trajectories as obtained from FLEXTRA (cf. Sect. 3.2; Stohl et al., 1995) which end at flight-time and altitude sections where NPF was observed along the flight path of the M-55 "Geophysica". In Fig. 5 the pathway of these trajectories towards the M-55 "Geophysica" flight tracks are displayed over 10 days prior to the measurement and colored according to the potential temperature along respective trajectory in order to illustrate the air mass vertical movement.

For new particle formation observed during the TROCCINOX flight (Case 1), two different air mass trajectories were considered. The first trajectory originates from the west coast of South America, i.e. Peru, and exhibits spatially extended and slow uplift towards the flight path (see Fig. 5). Most other trajectories for this NPF observation (Case 1) underwent convective lifting starting over the Pacific Ocean, more than 2500 km west of South America's coast (see Fig. 5). Due to oceanic emissions of dimethylsulfide (DMS, Charlson et al., 1987) which is oxidized to SO_2, the Pacific trajectories did not necessarily carry much less SO_2 compared to the Peruvian trajectory. The MAIA calculations for the two SCOUT-AMMA NPF observations (Cases 2 and 3, see Fig. 6c and d) are based on one air mass trajectory for each case. For the Case 2 and Case 3 trajectories the FLEXTRA calculations indicated recent convective uplift. For Case 2 the air mass originated over the African continent, in Central Sudan (see Fig. 5) moving at low level towards North Ethiopia and Eritrea before convective uplift

ACPD
11, 9249–9312, 2011

occurred over North Ethiopia 4 days before sampling (see Fig. 6c). In the North of Ethiopia (i.e. Dabbahu rifting zone of the Nubia–Arabia Plate boundary, Afar region) a volcanically active region is located (Hamling et al., 2009; Ferguson et al., 2010), and volcanic emission potentially contributed to the air mass SO_2 loading. As the trajectory narrowly passes also the Red Sea coast natural SO_2 sources (by DMS) or, as the Red Sea is a highly frequented route of sea going ships, a contribution of anthropogenic SO_2 emission is conceivable. According to the FLEXTRA calculations for Case 3 the origin of the air masses was over the Bay of Bengal 10 days earlier. The trajectory describes a cyclonic turn partly crossing Myanmar, Bangladesh and India while continuously ascending over land, reaching highest altitude about 4.5 days before the sampling. Thus, SO_2 from natural as well as anthropogenic sources over sea or of pollution from the Asian continent could have been transported into the TTL. This is in general agreement with Law et al. (2010) finding pollution sources in Asia influencing the TTL composition over Africa.

Table 2 provides a summary of the initial parameters for the MAIA runs. The values listed for water vapor, pressure, and temperature are derived from the FLEXTRA trajectories. The noon OH concentration represents the peak value in the parameterization of OH as a function of the cosine of the zenith angle. A zero OH concentration is assumed at nighttime. The ion pair production rate due to cosmic rays is calculated in the course of the MAIA runs (cf. Sect. 3.3). The SO_2 mixing ratio obtained from the FLEXPART model are likely overestimates because SO_2 loss processes are ignored. Additionally, the FLEXTRA and the MAIA calculations do not take into account that air masses are mixed and SO_2 is probably diluted. Therefore, for the separate MAIA runs, pre-existing SO_2 mixing ratios of 500 pptv (black lines in Fig. 6) and additionally a significantly lower value of 50 pptv (red lines in Fig. 6) were used as model input.

SO_2 mixing ratios in polluted industrial outflow measured in the boundary layer over the Bay of Bengal can reach values exceeding 1.5 ppbv (Lilieveld et al., 2001). Pollution emissions of SO_2 from Peruvian copper smelters were observed over 10 months to release a mean daily SO_2 burden of 0.2–3 Gg per day (Carn et al., 2007) and by a 6

ACPD
11, 9249–9312, 2011

month lasting study at a Peruvian measurement site (Marcapomacocha) a median SO_2 mixing ratio was determined to range at about 3 ppbv (Carmichael et al., 2003). Thus, even considering SO_2 loss during the transport into the TTL, it seems to be plausible that polluted air masses from Asia or Peru reach the TTL with a SO_2 mixing ratio which differs not too much from the upper limit of estimated pre-existing SO_2 mixing ratio for the MAIA simulations (i.e. 500 pptv). Contrary, the SO_2 loading of air masses over East Africa (Sudan, Ethiopia and Eritrea) or over the Pacific Ocean may be less intense, such that air masses with according transport history, when reaching the TTL, may contain significantly less SO_2 compared to previous cases, probably even close to the lower limit of assumed pre-existing SO_2 mixing ratio for the MAIA simulations (i.e. 50 pptv).

Since pre-existing surface area (in μm^2 per cm^3 of air) of the background aerosol constitutes a sink for gaseous H_2SO_4 and the highly mobile newly formed particles, five different simulations were performed, varying the initial aerosol surface area, using values of 0.5, 1, 2, 4, and 8 $\mu m^2\,cm^{-3}$. These aerosol surface area densities are kept constant during respective simulation run. The purpose of choosing a broad range as initial assumptions for the MAIA calculations is to compensate that mixing and dilution processes are underestimated by this approach. The results of these simulations are shown in Fig. 6. Each panel displays the number of ultrafine particles ($N_6 - N_{15}$) per cm^3 predicted by MAIA due to ion-induced and neutral nucleation as function of time. At time zero the air parcel was sampled by the instrumentation on board the aircraft.

For completeness, MAIA simulations were conducted to both trajectories for the TROCCINOX case (Case 1), along the Peruvian trajectory with spatially extended and slow uplift (Fig. 6a) and along the Pacific trajectory that underwent convective lifting to measurement altitudes (Fig. 6b). For the MAIA simulations concerning the separate SCOUT-AMMA cases the trajectory originating from East Africa (Case 2 – Fig. 6c) and the Bay of Bengal (Case Fig. 6d) are considered.

Notably, the increase of N_{uf} predicted by MAIA starts temporally staggered. The time that is needed for the formation of molecular clusters, for their growth to stable but very

ACPD
11, 9249–9312, 2011

small particles (1.5 nm) and for further growth until reaching sizes between 6–15 nm is governed by the abundance of gaseous H_2SO_4. Additionally, the number of formed clusters and small particles influence the time that is needed for particles to grow to N_{uf} sizes.

4.3.1 Results of the MAIA simulations for the NPF events

The maximum of NPF predicted by the nucleation model appears several days (e.g. up to 6.5 days, cf. Fig. 6b) before the actual measurement. The temporal evolution of N_{uf} strongly depends on the history of the respective trajectory, the pre-existing aerosol surface area, and the initial concentration of SO_2. The resulting number concentration N_{uf} at time zero predicts the quantity of ultrafine particles at the location of the flight track of the M-55 "Geophysica" where NPF has been detected by COPAS.

The aerosol nucleation model predicts maxima of N_{uf} due to NPF ranging up to 30 000–40 000 particles cm^{-3}. These values arise with 0.5 μm^2 cm^{-3} of pre-existing aerosol surface area and SO_2 concentrations of 500 pptv, i.e. under maximum available SO_2 and minimum background aerosol surface area. In contrast, if initial SO_2 concentrations of 50 pptv and a pre-existing aerosol surface area of 4.0 μm^2 per cm^3 are assumed then the MAIA model prediction excludes massive NPF to occur, resulting in negligible concentrations of ultrafine aerosol at the times of COPAS measurement (dotted red lines in Fig. 6). The contributions of neutral and charged nucleation to new particle formation as simulated by MAIA on the FLEXTRA trajectories depend mainly on temperature and sulfuric acid concentration in the gas phase. Generally, lower temperatures and higher sulfuric acid gas phase concentrations, which may arise either due to low pre-existing aerosol concentrations, high initial SO_2 levels, or both, favor neutral over charged nucleation, but the relative strengths of the two processes may change on a given trajectory along with environmental conditions. Therefore, no systematic bias towards either of the two nucleation processes exists on the considered trajectories, and either of the two processes may dominate depending on environmental

ACPD
11, 9249–9312, 2011

conditions. For example, low temperatures (205–234 K) along the FLEXTRA trajectory leading from the Pacific Ocean to the M-55 "Geophysica" flight track during the TROCCINOX flight on 24 February 2005 (MAIA results in Fig. 6b) lead to stronger neutral nucleation at 500 ppt SO_2 over most of the trajectory. On the other hand, on the FLEXTRA trajectory originating in Peru, with somewhat higher temperatures (209–238 K), charged nucleation prevails at 500 ppt SO_2 over most of the trajectory (MAIA results in Fig. 6a).

4.3.2 Contribution of the ion-induced mechanism to the NPF simulated by MAIA

In Fig. 7 the fractional contribution of the ion-induced mechanism is displayed along each of the MAIA runs that are shown in Fig. 6. The largest contribution of the ion-induced mechanism ranges at about 40–90% immediately prior and during the NPF bursts. After NPF bursts, correlated with sun zenith and the production maximum of OH, which is essential for processing SO_2 into H_2SO_4, the ion-induced mechanism is periodically active (in 24 h time steps) with a fractional contribution by 30–50%, occasionally peaking up to 60%. During night hours the neutral nucleation mechanism dominates the processing of the ultrafine particles. However, for those MAIA simulation runs, assuming 500 pptv of initial SO_2, neither the ion-induced nor the neutral nucleation mechanism seems to contribute to an effective increase of N_{uf} after the NPF burst. Under same precondition concerning initial SO_2 the predicted N_{uf}, generally, stagnates or decreases after the NPF burst. In those cases for which 50 pptv of initial SO_2 is assumed both mechanisms lead to an effective increase of predicted N_{uf} for which the ion-induced mechanism periodically contributes by, at least, 30–40%.

ACPD
11, 9249–9312, 2011

5 Discussion

5.1 Case 1 – 24 February 2005

For Case 1 the MAIA calculation on the Peruvian trajectory (Fig. 6a) predicts number concentrations of ultrafine particles ranging from 600–3000 per cm^3 at the intersection with the flight track. With the higher initial SO_2 concentration (500 pptv), the concentration of ultrafine aerosol N_{uf} peak early on the trajectory for all considered initial aerosol surface area concentrations (black curves in Fig. 6a). Following this peak, N_{uf} values gradually decrease due to coagulation of the particles, and due to their growth out of the size interval covered by N_{uf}. At the time of the measurement, the simulations with 500 pptv of initial SO_2 significantly underpredict the observed aerosol concentration, regardless of the initial aerosol surface area concentration.

With 50 pptv of initial SO_2 (red curves in Fig. 6a), new particle formation is strongly suppressed at initial aerosol surface area concentrations $\geq 4\,\mu m^2\,cm^{-3}$. However, with decreasing initial aerosol surface area concentrations, NPF becomes more efficient, and for pre-existing aerosol surface area concentrations $\leq 1\,\mu m^2\,cm^{-3}$, 50 pptv of initial SO_2 gives concentrations of ultrafine aerosol at the time of the measurements that match the observations better than any of the 500 pptv runs.

Similar results are obtained on the trajectory arriving from the Pacific (Fig. 6b): here, however, more time has passed since the initial uplift compared to the Peruvian trajectory, and the newly formed particles have had more time to coagulate and grow out of the size interval covered by N_{uf} (see Sect. 2.2). As a result, along this trajectory the model predicts particle concentrations that are significantly lower than the observations at the time of the measurement, as well as the concentrations produced on the Peruvian trajectory.

The conclusions which can be drawn from these results are: The better match between modeled and observed N_{uf} from NPF is obtained with a low initial SO_2, which indicates that in the considered cases, the observed N_{uf} is mainly governed by the pre-existing aerosol surface area rather than by air parcels rich in SO_2. If the aerosol

ACPD
11, 9249–9312, 2011

surface area is low enough (e.g. as a result of cloud processing) then a better agreement between the MAIA-simulated and the observed number density of ultrafine particles is reached. While cloud processing reduces in different ways both, aerosol and SO_2 concentrations, a reduction of aerosol surface area can more than compensate a reduction of SO_2, and explain observed particle concentrations, as seen in the simulations. This is supported by the finding that high SO_2 concentrations deteriorate the comparison of the simulations with the measurements. High SO_2 concentrations lead to a rapid growth of the newly formed particles out of the ultrafine particle size regime. Furthermore, the better match between measured and modeled N_{uf} obtained on the Peruvian trajectory, compared to the Pacific trajectory, confirms that NPF which resulted in the observed concentration of ultrafine aerosol has most likely taken place in air parcels originating from Peru.

5.2 Case 2 – 7 August 2006

For the NPF Case 2 (Fig. 6c), MAIA reproduces the COPAS ultrafine particle measurement quite well with N_{uf} around 4000 particles per cm^3, provided that the lower initial SO_2 mixing ratio of 50 pptv and a very low initial aerosol surface area concentration ($\leq 1\,\mu m^2\,cm^{-3}$) are assumed. Higher aerosol surface areas or a high initial SO_2 mixing ratio give lower simulated particle concentrations at the time of the measurement. This is indicative of efficient cloud processing along the trajectory, e.g. in deep convection. Given the FLEXPART prediction of 1.4 ppbv SO_2 for this trajectory (see Fig. 4b at 14:15 UTC), efficient cloud processing appears very likely if the SO_2 is to be reduced to values around 50 pptv. Again, uncertainties in the EDGAR inventory and the unquantified losses and dilution of SO_2 due to cloud related processes and mixing with background air in the TTL may well be the cause of the corresponding differences.

ACPD
11, 9249–9312, 2011

5.3 Case 3 – 7 August 2006

The predicted number densities of ultrafine particles for NPF Case 3 (Fig. 6d) range between 3000–4000 particles per cm^3 for the simulations with initial SO_2 concentrations of 500 pptv, and exceed the value of 1300 per cm^3 determined by COPAS. For 50 pptv SO_2 and $\leq 1\,\mu m^2\,cm^{-3}$ of pre-existing aerosol surface area, the MAIA results coincide with those from the runs with 500 pptv. At 50 pptv initial SO_2 concentration and $0.5\,\mu m^2\,cm^{-3}$ pre-existing aerosol surface area, the model predicts a significantly higher particle concentration, while for aerosol surface area $>1\,\mu m^2\,cm^{-3}$, N_{uf} remains low with values $\sim 100\,cm^{-3}$ or below. Cloud processing appears not to be required to explain the observed concentrations of ultrafine particles in this case, as a range of initial conditions in the MAIA simulation explains the observed particle concentration.

5.4 Case study upshot

Generally, the number concentration of ultrafine particles predicted by the MAIA nucleation model compare well with the N_{uf} measured by COPAS during observed NPF events. The remaining differences between the model predictions and the observations may be due to:

1. the uncertainty of the air mass trajectory calculations by the FLEXTRA model, particularly the uncertainties in the representation of (local) convection,
2. the uncertainties in the source strengths for SO_2,
3. for NPF Case 3 the unquantified losses of SO_2 inside clouds (which may play a significant role given in the very large MCS that were regularly present during the West African monsoon season of 2006),
4. the uncertainties in the MAIA model assumptions (constant surface area densities, the non-consideration of air mass mixing/dilution as well as SO_2 processing) or

ACPD
11, 9249–9312, 2011

5. the contribution of nucleating and condensable species not accounted for by MAIA, such as organic compounds (Heald et al., 2005; Kulmala et al., 2006; Ekman et al., 2008).

Nevertheless, the results indicate that a low pre-existing aerosol surface area is an essential prerequisite for NPF within the upper troposphere.

The MAIA nucleation model simulations concerning these NPF cases were based on assumptions of initial SO_2 concentration and preexisting aerosol surface area, and account only for nucleation of H_2SO_4-H_2O aerosol particles. These assumptions lead to MAIA predictions of the number of ultrafine particles mostly in reasonable agreement with in situ observation without considering a nucleation mechanism involving organic components.

However, in Fig. 8 the N_{uf} is displayed versus the CO mixing ratio measured during the flight on 7 August 2006 over West Africa. Data points are color-coded according to the potential temperature. Those N_{uf} which were measured during NPF Case 2 and Case 3 are highlighted separately. CO mixing ratios with more than 60 ppbv were generally observed below 380 K potential temperature which is below the cold point tropopause. Particularly such NPF events that result in N_{uf} of more than 400 particles per cm^3 seem to occur when the analyzed air masses are CO enriched (typical CO background levels are 60–70 ppb in the pristine marine boundary layer). For mildly elevated CO levels in the range between 67 and 82 ppbv, concentrations of ultrafine particles (N_{uf}) frequently assumed values of up to 4000 particles per cm^3, although the absence of NPF was observed as well. Higher CO mixing ratios in the range 82–93 ppbv were measured almost exclusively during NPF events. The largest amount of N_{uf} (~5400 particles per cm^3) during the flight on 7 August was observed along with >90 ppbv of CO at $350\,K < \Theta < 360\,K$.

Law et al. (2010) found air masses containing elevated CO (concurrently with O_3, CO_2, and NO_y) which were likely influenced by pollution emissions over Asia and India and which underwent a long range transport towards the TTL over West Africa. Law et al. (2010) describe that this way ~40% of the air masses reaching the 355 K level

ACPD
11, 9249–9312, 2011

over West Africa during SCOUT-AMMA (~20% at the 370 K level) might have been impacted by pollution from Asia and India. Pollution emissions are also coupled with the release of components such as SO_2 and gaseous organic substances as well as organic aerosols (Lelieveld et al., 2001). Thus, significant amounts of gaseous organic compounds, as potential NPF precursors, from Asian pollution could have been carried aloft towards the African TTL. Therefore, it cannot be excluded that nucleation of organic compounds contributed to the observed NPF. More detailed conclusions, particularly concerning specific organic species which probably influence the NPF in the TTL region, or if, as Kulmala et al. (2006) suggest, the nucleation mechanism of organic compounds are dominant, cannot be reached here as the M-55 "Geophysica" was not equipped with any instrumentation determining the aerosol chemical composition or gas phase organic compounds.

5.5 NPF inside clouds

5.5.1 In-cloud NPF over Brazil (Case 1)

During the TROCCINOX NPF Case 1 the ultrafine particles almost disappear (N_{uf} as low as 40 cm^{-3}) when the aircraft is flying within a cirrus cloud (as indicated by the FSSP-100 data for $N_{>2\,\mu m}$ in Fig. 3a) between 14:13:20 and 14:16:40 UTC. The number concentration of ice particles with $d_p > 2\,\mu m$ reached up to 1.1 cm^{-3} (0.1 cm^{-3} in average) and the cloud particle size distribution is given in Fig. 9 by the light green curve (Note: No CIP was available during TROCCINOX). More details, for Case 1 are provided in Table 2 as averages over the time of the cloud encounter. The particle surface area of the cirrus cloud over South America is significantly smaller compared to observations over West Africa. This is due to the fact that for Case 1 the particle surface area was exclusively obtained from FSSP-100: particles larger than the upper size limit of the instrument (i.e. $d_p > 30\,\mu m$) could not be detected even though they probably were present. Judging from the shape of the size distribution in Fig. 9, however, it is plausible that the number densities of the larger ice particles in Case 1 were

ACPD
11, 9249–9312, 2011

significantly below those of the other clouds, and hence that the total ice surface area observed over South America was indeed lower than over West Africa.

5.5.2 In-cloud NPF over West Africa (Cases 2 and 3)

Figure 10 shows a close-up of the time series of the SCOUT-AMMA NPF Cases 2 and 3 according cloud particle size distributions are shown in Fig. 9. In Case 2 the M-55 "Geophysica" crossed a thin cirrus layer (labeled as Ice-cloud I in Fig. 10) at ~12.5 km altitude (14:12:18–14:13:31 UTC) with average ice particle concentrations of 0.4 cm^{-3}, a maximum number density of 1.3 cm^{-3}, particle surface areas around 3.5×10^6 µm cm^{-3} and an aerosol volume backscatter coefficient of 1.6×10^{-6} m^{-1} sr^{-1} with depolarization of 62% (see Fig. 3b, Table 2, and black curve in Fig. 10). The highest concentration of freshly nucleated ultrafine particles N_{uf} in this cloud ranges up to and 4000 particles per cm^3. During NPF Case 3 two cirrus clouds were encountered in connection with the anvil outflow of a West African MCS (as described in Frey et al., 2011). First a thin cirrus layer was passed at ~13 km altitude (15:36:09–15:37:32, marked as Ice-cloud II) with ice particle concentrations up to 0.9 cm^{-3}, at 0.3 cm^{-3} on average. A denser cirrus cloud was crossed at ~12 km altitude (15:38:00–15:42:36, denoted with Ice-cloud III), where $N_{>2\,\mu m}$ of up to 8.3 cm^{-3} (4.4 cm^{-3} in average) was detected by the FSSP-100 (see Fig. 3b). At the time when the maximum cloud particle concentration in Ice-cloud II was detected, N_{uf} still ranged between 1100 and 630 particles per cm^3. For Ice-cloud III a first size distribution is reported from the cloud edge region (blue curve in Fig. 9). Here, N_{uf} was still about 760 particles per cm^3. Well inside Ice-cloud III, the ultrafine particles vanish and N_{uf} decreased to zero (Fig. 10). Notably, the ice particle size distribution dN/dlog d_p (dark cyan curve in Fig. 9) exhibits the highest values encountered during SCOUT-AMMA. At the same time, the aerosol volume backscatter coefficient as well as the cloud particle volume depolarization increased significantly. After exiting Ice-cloud III, N_{uf} recovered to concentrations between 170–1500 ultrafine particles per cm^3 (Fig. 10).

ACPD
11, 9249–9312, 2011

5.5.3 Intercomparison and interpretation

The cloud particle size distributions during the in-cloud NPF cases are very similar for Ice-clouds I and II, as well as for the edge region of Ice-cloud III. The measurements of the MAS instrument suggest that the aerosol volume backscatter coefficient as well as the depolarization remains nearly constant for Ice-cloud I, II, and the edge of Ice-cloud III, which indicates that the particle shape (crystal habit) and cloud element sizes did not significantly change from one ice cloud to the other. However, deeper inside Ice-cloud III, with high ice crystal surface area concentrations, N_{uf} values were significantly reduced compared to the other ice clouds.

The occurrence of ultrafine aerosol particles inside cirrus clouds has been previously reported by Lee et al. (2004). Kazil et al. (2007) have shown that aerosol nucleation inside cirrus clouds is possible and more viable at small ice and aerosol surface area concentrations. Alternatively, ultrafine aerosol particles inside cirrus clouds could arise due to aerosol nucleation in cloud-free air and subsequent cirrus formation, by sedimentation of cirrus ice crystals into an air mass in which NPF occurred, or by turbulent mixing of air parcels that contain ultrafine aerosol and ice crystals. From our observations in West Africa it can be concluded that in the presence of ice cloud particles ($d_p > 2\,\mu m$) at concentrations of $\sim 2\,cm^{-3}$ or less, ultrafine particles can form or persist in significant amounts. However, the NPF Case 1, observed over South America, also demonstrates that the presence of cirrus clouds with much lower ice particle concentrations suppresses the formation or presence of ultrafine aerosol. Uncovering the mechanisms giving rise to the presence and possibly to the formation of ultrafine aerosol particles inside cirrus clouds will require detailed measurements of gas phase composition, and of aerosol and ice particle size distributions in and around cirrus.

ACPD
11, 9249–9312, 2011

6 Summary and conclusions

Enhanced abundances of aerosol in the ultrafine size range, detected by aircraft borne in situ measurements in the tropical continental free troposphere and TTL region over West Africa and Brazil, which indicate recent new particle formation, are presented. Number concentrations of such particles as high as 7700 cm^{-3} were measured at ~12.5 km altitude over South America (24 February 2005) and up to 4000 cm^{-3} at ~13.0 km over West Africa (7 August 2006), one NPF event observed at ~13.7 km over South America even peaks to >16 000 ultrafine particles per cm^3 (27 January 2005). The occurrence of new particle formation at half of all flights over South America and during each local flight over West Africa was confined to a layer between 340 K and 370 K potential temperature. This potential temperature range covers the tropical upper troposphere (UT) and the Tropical Transition Layer (TTL). Except for one case, no significant new particle formation was encountered in the stratosphere. The detected ultrafine, freshly nucleated particles were to large quantities volatile when heated to 250 °C during sampling. The sampling of particles after heat exposure primarily aims at vaporizing H_2SO_4-H_2O aerosol compounds, this way, however, also aerosol compounds of higher volatility (e.g. organics) are vaporized. The highest amounts of newly formed particles and the longest duration of NPF events in the UT/TTL were found between 350–370 K potential temperature over Brazil and West Africa. This indicates that NPF occurs as strongest above the convective outflow regions of the upper troposphere and in the lowest part of the TTL.

Numerical simulations with the aerosol nucleation model MAIA predict formation of ultrafine aerosol particles from the gas phase in numbers that compare reasonably well with the observations. Since MAIA treats only neutral and charged nucleation of H_2SO_4-H_2O particles, this result indicates that the resulting particle number concentration of NPF could be appropriately predicted exclusively due to nucleation of sulfuric acid and water. However, measurements over West Africa exhibit elevated concentrations of CO during NPF events. Here, the back trajectories point towards contributions

ACPD
11, 9249–9312, 2011

of anthropogenic emissions of pollution material from Asia. Therefore, it is plausible, though it cannot be proven by measurements, that water insoluble organic compounds contributed to the new particle formation to some, not further quantifiable, extent. The MAIA calculations suggest that the absolute strength of NPF events – the maximum of freshly formed particles during NPF bursts – is strongly influenced by the availability of fresh H_2SO_4 emanating from SO_2. As ultrafine particles in burst-like events of NPF (due to high SO_2 loading) rapidly coagulate and grow, the MAIA simulations based on small amounts of SO_2 results in slower but longer lasting formation of new ultrafine particles, as a function of time, in similar or even higher quantities.

Nucleation mode particles were detected not only in clear air but also within thin cirrus cloud layers, indicating that new particle formation occurred in both, clear air, as well as in clouds. Alternatively, mixing of cloud-free and cloudy air parcels, aerosol nucleation and cirrus formation occurring in sequence, and ice particles which had sedimented into an air parcel where aerosol nucleation had occurred could explain the observation of ultrafine aerosol inside cirrus clouds. Ultrafine aerosol particles were found at very low concentrations inside cirrus cloud segments where the total number concentration of cloud particles (within a size range of 2.7µm < d_p < 1.6 mm) exceeded 2 cm^{-3}. In-cloud (cirrus) NPF in the tropical UT can be envisaged, if sufficient amounts of NPF precursors from the boundary layer are carried aloft by deep convection. Despite significant removal of the gaseous precursors by scavenging during the upward transport, enough gaseous material may remain inside the Cb anvil and its outflow for enabling NPF.

If the ultrafine particles do not immediately disappear within clouds, one could speculate that a high frequency of such NPF events could well be the major reason for the belt of enhanced number densities of small particles in the 340 K to 390 K altitude range described by Brock et al. (1995). The significantly decreased number densities of particles containing non-volatile cores (Borrmann et al., 2010) – with the implication of higher abundances of volatile solution droplets – support this notion. If NPF occurs, as our data seem to indicate, in a remarkably narrow altitude range at the bottom of the

ACPD
11, 9249–9312, 2011

TTL, then the outflows of Cb clouds and MCS may turn out to be a major contributor, as a supplier of NPF precursor substances into the TTL. This contribution might significantly add to the new particle formation in clear air. However, because the air between the clouds in the tropical upper troposphere must have a descending component – in compensation for the rapid convective ascent inside Cbs – ultrafine aerosol particles produced by NPF in clear air may even have a reduced chance of being carried aloft into the stratosphere. On the other hand, since many of the tropical convective clouds reach the bottom part of the TTL, freshly nucleated aerosol particles in their anvil outflows have the potential to directly enter the radiatively driven slow ascent from the TTL towards the stratosphere. This potentially strengthens the role of the tropical clouds in particular, and the UT and TTL in general as source regions for the stratospheric aerosol population.

Beyond such speculative considerations the particles that are newly formed in the tropical UT and lowermost TTL, immediately above the main outflow level of the tropical convection, are of particular importance in the light of the Brock et al. (1995) hypothesis, according to which the tropical TTL acts as major source regions for the global lower stratospheric aerosol and the Junge layer.

Acknowledgements. The TROCCINOX and SCOUT-O3 projects were funded by the EC under Contracts No. EVK2-CT-2001-00122 and 505390-GOCE-CT-2004-505390. The M-55 "Geophysica" campaigns also were supported by the EEIG-Geophysica Consortium, CNRS-INSU, EC Integrated Projects AMMA-EU (Contract No. 004089-2), and by DLR. Based on a French initiative, AMMA was funded by several research agencies from France, the United Kingdom, the United States, Africa, Germany, and in particular from the European Community Sixth Framework Program (AMMA-EU). For us significant support also was provided from the Max-Planck-Society. Also we acknowledge logistical support from the AMMA Operations Centre in Niamey, Niger. The local authorities, scientists, and staff in Araçatuba (Brazil), and Ouagadougou (Burkina Faso) were extraordinarily helpful for conducting the campaigns. We thank T. Drabo (Ouagadougou), S. Balestri and the entire M-55 "Geophysica" crew, especially the pilots and engineers. Essential technical support for our instruments was provided by T. Böttger, W. Schneider, C. von Glahn, and M. Flanz, and is most gratefully acknowledged.

ACPD
11, 9249–9312, 2011

H. Rüba, T. Hamburger and B. Weinzierl are acknowledged for supporting the CPC measurements aboard the DLR Falcon-20. We thank U. Schumann (DLR) for the coordination and the flight planning during TROCCINOX. J. Kazil is supported by the NOAA OAR Climate Program Office grant NA08OAR4310566. The flight missions of the NASA WB-57F aircraft (Pre-AVE, AVE_0506, Cr-AVE and TC4) in the years 2004 to 2007 during which the University of Denver NMASS instrument participated in has been supported by the NASA Earth Science Division.

References

Barth, M. C., Stuart, A. L., and Skamarock, W. C.: Numerical simulations of the July 10, 1996, Stratospheric-Tropospheric Experiment: Radiation, Aerosols, and Ozone (STEREAO)-Deep Convection experiment storm: Redistribution of soluble tracers, J. Geophys. Res., 106, 12381–12400, 2001.

Borrmann, S., Kunkel, D., Weigel, R., Minikin, A., Deshler, T., Wilson, J. C., Curtius, J., Volk, C. M., Homan, C. D., Ulanovsky, A., Ravegnani, F., Viciani, S., Shur, G. N., Belyaev, G. V., Law, K. S., and Cairo, F.: Aerosols in the tropical and subtropical UT/LS: in-situ measurements of submicron particle abundance and volatility, Atmos. Chem. Phys., 10, 5573–5592, doi:10.5194/acp-10-5573-2010, 2010.

Brock, C. A., Hamill, P., Wilson, J. C., Jonsson, H. H., and Chan, K. R.: Particle Formation in the Upper Tropical Troposphere - a Source of Nuclei for the Stratospheric Aerosol, Science, 270(5242), 1650–1653, 1995.

Brock, C. A., Schröder, F., Kärcher, B., Petzold, A., Busen, R., and Fiebig, M.: Ultrafine particle size distributions measured in aircraft exhaust plumes, J. Geophys. Res.-Atmos., 105(D21), 26555–26567, 2000.

Brown, P. N., Byrne, G. D., and Hindmarsh, A. C.: VODE, A Variable-Coefficient ODE Solver, SIAM J. Sci. Stat. Comput., 10, 1038—1051, 1989.

Buontempo, C., Cairo, F., Di Donfrancesco, G., Morbidini, R., Viterbini, M., and Adriani, A.: Optical measurements of atmospheric particles from airborne platforms: in situ and remote sensing instruments for balloons and aircrafts, Ann. Geophys.-Italy, 49, 57–64, 2006.

Cairo, F., Pommereau, J. P., Law, K. S., Schlager, H., Garnier, A., Fierli, F., Ern, M., Streibel, M., Arabas, S., Borrmann, S., Berthelier, J. J., Blom, C., Christensen, T., D'Amato, F., Di Donfrancesco, G., Deshler, T., Diedhiou, A., Durry, G., Engelsen, O., Goutail, F., Harris, N.

ACPD
11, 9249–9312, 2011

R. P., Kerstel, E. R. T., Khaykin, S., Konopka, P., Kylling, A., Larsen, N., Lebel, T., Liu, X., MacKenzie, A. R., Nielsen, J., Oulanowski, A., Parker, D. J., Pelon, J., Polcher, J., Pyle, J. A., Ravegnani, F., Rivire, E. D., Robinson, A. D., Röckmann, T., Schiller, C., Simões, F., Stefanutti, L., Stroh, F., Some, L., Siegmund, P., Sitnikov, N., Vernier, J. P., Volk, C. M., Voigt, C., von Hobe, M., Viciani, S., and Yushkov, V.: An introduction to the SCOUT-AMMA stratospheric aircraft, balloons and sondes campaign in West Africa, August 2006: rationale and roadmap, Atmos. Chem. Phys., 10, 2237–2256, doi:10.5194/acp-10-2237-2010, 2010.

Cairo, F., Di Donfrancesco, G., Snels, M., Fierli, F., Viterbini, M., Borrmann, S., and Frey, W.: A comparison of light backscattering and particle size distribution measurements in tropical cirrus clouds, Atmos. Meas. Tech., 4, 557–570, doi:10.5194/amt-4-557-2011, 2011.

Carmichael, G. R., Ferm, M., Thongboonchoo, N., Woo, J.-H., Chan, L. Y., Murano, K., Viet, P. H., Mossberg, C., Bala, R., Boonjawat, J., Upatum, P., Mohan, M., Adhikary, S. P., Shrestha, A. B., Pienaar, J. J., Brunke, E. B., Chen, T., Jie, T., Guoan, D., Peng, L. C., Dhiharto, S., Harjanto, H., Jose, A. M., Kimani, W., Kirouane, A., Lacaux, J.-P., Richard, S., Barturen, O., Cerda, J. C., Athayde, A., Tavares, T., Cotrina, J. S., and Bilici, E.: Measurements of sulfur dioxide,ozone and ammonia concentrations in Asia, Africa, and South America using passive samplers, Atmos. Environ., 37, 1293–1308, doi:10.1016/S1352-2310(02)01009-9, 2003.

Carn, S. A., Krueger, A. J., Krotkov, N. A., Yang, K., and Levelt, P. F.: Sulfur dioxide emissions from Peruvian copper smelters detected by the Ozone Monitoring Instrument, Geophys. Res. Lett., 34, L09801, doi:10.1029/2006GL029020, 2007.

Charlson, R. J., Lovelock, J. E., Andreae, M. O., and Warren, S. G.: Oceanic phytoplankton, atmospheric sulphur, cloud albedo and climate, Nature, 326, 655–661, 1987.

Clarke, A. D., Eisele, F., Mauldin, R. L., Tanner, D., and Litchy, M.: Particle production in the remote marine atmosphere: Cloud outflow and subsidence during ACE 1, J. Geophys. Res.-Atmos., 103(D13), 16397–16409, 1998.

Clarke, A. D., Clarke, A. D., Eisele, F., Kapustin, V. N., Moore, K., Tanner, D., Mauldin, R. L., Litchy, M., Lienert, B., Carrol, M. A., and Albercook, G.: Nucleation in the equatorial free troposphere: Favorable environments during PEM-Tropics, J. Geophys. Res.-Atmos., 104(D5), 5735–5744, 1999.

Clarke, A. D. and Kapustin, V. N.: A pacific aerosol survey. Part I: A decade of data on particle production, transport, evolution, and mixing in the troposphere, J. Atmos. Sci., 59(3), 363–382, 2002.

Clegg, S. L., Rard, J. A., and Pitzer, K. S.: Thermodynamic properties of 0-6 mol kg-1 aque-

ACPD
11, 9249–9312, 2011

ous sulfuric acid from 273.15 to 328.15 K, J. Chem. Soc., Faraday Trans., 90, 1875–1894, doi:10.1039/FT9949001875, 1994.
Curtius, J., Froyd, K. D., and Lovejoy, E. R.: Cluster Ion Thermal Decomposition (I): Experimental Kinetics Study and ab Initio Calculations for HSO4-(H2SO4)x(HNO3)y, J. Phys. Chem. A, 105(48), 10867–10873, 2001a.
Curtius, J., Sierau, B., Arnold, F., de Reus, M., Ström, J., Scheeren, H. A., and Lelieveld, J.: Measurement of aerosol sulfuric acid 2. Pronounced layering in the free troposphere during the second Aerosol Characterization Experiment (ACE 2), J. Geophys. Res.-Atmos., 106(D23), 31975–31990, 2001b.
Curtius, J., Weigel, R., Vössing, H.-J., Wernli, H., Werner, A., Volk, C.-M., Konopka, P., Krebsbach, M., Schiller, C., Roiger, A., Schlager, H., Dreiling, V., and Borrmann, S.: Observations of meteoric material and implications for aerosol nucleation in the winter Arctic lower stratosphere derived from in situ particle measurements, Atmos. Chem. Phys., 5, 3053–3069, doi:10.5194/acp-5-3053-2005, 2005.
Curtius, J.: Nucleation of atmospheric aerosol particles, C. R. Physique, 7, 1027–1045, 2006.
Curtius, J., Lovejoy, E. R., and Froyd, K. D.: Atmospheric ion-induced aerosol nucleation, Space Sci. Rev., 125(1–4), 159–167, 2006.
Crumeyrolle, S., Manninen, H. E., Sellegri, K., Roberts, G., Gomes, L., Kulmala, M., Weigel, R., Laj, P., and Schwarzenboeck, A.: New particle formation events measured on board the ATR-42 aircraft during the EUCAARI campaign, Atmos. Chem. Phys., 10, 6721–6735, doi:10.5194/acp-10-6721-2010, 2010.
Dye, J. E. and Baumgardner, D.: Evaluation of the Forward Scattering Spectrometer Probe. Part I: Electronic and optical studies, J. Atmos. Oceanic Technol., 1, 329–344, 1984.
de Reus, M., Borrmann, S., Bansemer, A., Heymsfield, A. J., Weigel, R., Schiller, C., Mitev, V., Frey, W., Kunkel, D., Kürten, A., Curtius, J., Sitnikov, N. M., Ulanovsky, A., and Ravegnani, F.: Evidence for ice particles in the tropical stratosphere from in-situ measurements, Atmos. Chem. Phys., 9, 6775–6792, doi:10.5194/acp-9-6775-2009, 2009.
Eichkorn, S., Wilhelm, S., Aufmhoff, H., Wohlfrom, K. H., and Arnold, F.: Cosmic ray-induced aerosol-formation: First observational evidence from aircraft-based ion mass spectrometer measurements in the upper troposphere, Geophys. Res. Lett., 29, 1698, doi:10.1029/2002GL015044, 2002.
Ekman, A. M. L., Krejci, R., Engström, A., Ström, J., de Reus, M., Williams, J., and Andreae, M. O.: Do organics contribute to small particle formation in the Amazonian upper troposphere?,

ACPD
11, 9249–9312, 2011

Geophys. Res. Lett., 35, L17810, doi:10.1029/2008GL034970, 2008.
Emanuel, K. A. and Živković-Rothman, M.: Development and evaluation of a convection scheme for use in climate models, J. Atmos. Sci., 56, 1766–1782, 1999.
Fiebig, M., Stein, C., Schröder, F., Feldpausch, P., and Petzold, A.: Inversion of data containing information on the aerosol particle size distribution usingmultiple instruments, J. Aerosol Sci., 36, 1353–1372, 2005.
Fierli, F., Orlandi, E., Law, K. S., Cagnazzo, C., Cairo, F., Schiller, C., Borrmann, S., Di Donfrancesco, G., Ravegnani, F., and Volk, C. M.: Impact of deep convection in the tropical tropopause layer in West Africa: in-situ observations and mesoscale modelling, Atmos. Chem. Phys., 11, 201–214, doi:10.5194/acp-11-201-2011, 2011.
Forster, C., Stohl, A., and Seibert, P.: Parameterization of convective transport in a Lagrangian particle dispersion model and its evaluation, J. Appl. Met. Clim., 46, 403–422, 2007.
Frey, W., Borrmann, S., Kunkel, D., Weigel, R., de Reus, M., Schlager, H., Roiger, A., Voigt, C., Hoor, P., Curtius, J., Krämer, M., Schiller, C., Volk, C. M., Homan, C. D., Fierli, F., Di Donfrancesco, G., Ulanovsky, A., Ravegnani, F., Sitnikov, N. M., Viciani, S., D'Amato, F., Shur, G. N., Belyaev, G. V., Law, K. S., and Cairo, F.: In-situ measurements of tropical cloud properties in the West African monsoon: upper tropospheric ice clouds, mesoscale convective system outflow, and subvisual cirrus, Atmos. Chem. Phys. Discuss., 11, 745–812, doi:10.5194/acpd-11-745-2011, 2011.
Froyd, K. D. and Lovejoy, E. R.: Experimental Thermodynamics of Cluster Ions Composed of H_2SO_4 and H_2O. 1. Positive Ions, J. Phys. Chem. A, 107(46), 9800–9811, 2003a.
Froyd, K. D. and Lovejoy, E. R.: Experimental Thermodynamics of Cluster Ions Composed of H2SO4 and H2O. 2. Measurements and ab Initio Structures of Negative Ions, J. Phys. Chem. A, 107, 46, 9812–9824, 2003b.
Froyd, K. D., Murphy, D. M., Lawson, P., Baumgardner, D., and Herman, R. L.: Aerosols that form subvisible cirrus at the tropical tropopause, Atmos. Chem. Phys., 10, 209–218, doi:10.5194/acp-10-209-2010, 2010.
Fuchs, N. A.: The Mechanics of Aerosols, translated from the Russian edition (Moscow) by R. E. Daisley and Marina Fuchs, edited by: Davies, C. N., 408 pp., Pergamon Press, London, Macmillan, New York, 1964.
Fueglistaler, S., Dessler, A. E., Dunkerton, T. J., Folkins, I., Fu, Q., and Mote, P. W.: Tropical Tropopause Layer, Rev. Geophys., 47, RG1004, doi:10.1029/2008RG000267, 2009.
Ferguson,D. J., Barnie,T. D., Pyle, D. M., Oppenheimer, C., Yirgu,G., Lewi, E., Kidane, T., Carn,

ACPD
11, 9249–9312, 2011

S., and Hamling, I.: Recent rift-related volcanism in Afar, Ethiopia, Earth. Planet. Sc. Lett., 292(3–4), 409–418, doi:10.1016/j.epsl.2010.02.010., 2010.
Gettelman, A., de F. Forster, P. M., Fujiwara, M., Fu, Q., Vomel, H., Gohar, L. K., Johanson, C., and Ammerman, M.: Radiation balance of the tropical tropopause layer, J. Geophys. Res., 109, D07103, doi:10.1029/2003JD004190, 2004.
Giauque, W. F., Hornung, E. W., Kunzler, J. E., and Rubin, T. T.: The thermodynamic properties of aqueous sulfuric acid solutions and hydrates from 15 to 300 K, Am. Chem. Soc. J., 82, 62–70, 1960.
Hamill, P., Jensen, E. J., Russell, P. B., and Bauman, J. J.: The life cycle of stratospheric aerosol particles, B. Am. Meteorol. Soc., 78(7), 1395–1410, 1997.
Hamling, I. J., Ayele, A., Bennati, L., Calais, E., Ebinger, C. J., Keir, D., Lewi, E., Wright, T. J., and Yirgu, G.: Geodetic observations of the ongoing Dabbahu rifting episode: new dyke intrusions in 2006 and 2007, Geophys. J. Int., 178(2), 989–1003, doi:10.1111/j.1365-246X.2009.04163.x, 2009.
Hanson, D. R. and Lovejoy, E. R.: Measurement of the thermodynamics of the hydrated dimer and trimer of sulfuric acid, J. Phys. Chem. A, 110(31), 9525–9528, doi:10.1021/jp062844w, 2006.
Heald, C. L., Jacob, D. J., Park, R. J., Russell, L. M., Huebert, B. J., Seinfeld, J. H., Liao, H., and Weber, R. J.: A large organic aerosol source in the free troposphere missing from current models, Geophys. Res. Lett., 32(18), L18809, doi:10.1029/2005GL023831, 2005.
Hermann, M., Heintzenberg, J., Wiedensohler, A., Zahn, A., Heinrich, G., and Brenninkmeijer, C. A. M.: Meridional distributions of aerosol particle number concentrations in the upper troposphere and lower stratosphere obtained by Civil Aircraft for Regular Investigation of the Atmosphere Based on an Instrument Container (CARIBIC) flights, J. Geophys. Res.-Atmos., 108(D3), 4114, doi:4110.1029/2001JD001077, 2003.
Hermann, M., Adler, S., Caldow, R., Stratmann, F., and Wiedensohler, A.: Pressure-dependent efficiency of a condensation particle counter operated with FC-43 as working fluid, J. Aerosol Sci., 36(11), 1322–1337, 2005.
Homan, C. D., Volk, C. M., Kuhn, A. C., Werner, A., Baehr, J., Viciani, S., Ulanovski, A., and Ravegnani, F.: Tracer measurements in the tropical tropopause layer during the AMMA/SCOUT-O3 aircraft campaign, Atmos. Chem. Phys., 10, 3615–3627, doi:10.5194/acp-10-3615-2010, 2010.
Huntrieser, H., Feigl, C., Schlager, H., Schröder, F., Gerbig, C., van Velthoven, P., Flatøy, F.,

ACPD
11, 9249–9312, 2011

Théry, C., Petzold, A., Höller, H., Schumann, U., Airborne measurements of NO_x, tracer species and small particles during the European Lightning Nitrogen Oxides Experiment, J. Geophys. Res.-Atmos., 107(11), 4113, doi:10.1029/2000JD000209, 2002.
Kazil, J. and Lovejoy, E. R.: Tropospheric ionization and aerosol production: A model study, J. Geophys. Res.-Atmos., 109(D19), D19206, doi:19210.11029/12004JD004852, 2004.
Kazil, J., Lovejoy, E. R., Barth, M. C., and O'Brien, K.: Aerosol nucleation over oceans and the role of galactic cosmic rays, Atmos. Chem. Phys., 6, 4905–4924, doi:10.5194/acp-6-4905-2006, 2006.
Kazil, J., Lovejoy, E. R., Jensen, E. J., and Hanson, D. R.: Is aerosol formation in cirrus clouds possible?, Atmos. Chem. Phys., 7, 1407–1413, doi:10.5194/acp-7-1407-2007, 2007.
Kerminen, V.-M., Petäjä, T., Manninen, H. E., Paasonen, P., Nieminen, T., Sipilä, M., Junninen, H., Ehn, M., Gagné, S., Laakso, L., Riipinen, I., Vehkamäki, H., Kurten, T., Ortega, I. K., Dal Maso, M., Brus, D., Hyvärinen, A., Lihavainen, H., Leppä, J., Lehtinen, K. E. J., Mirme, A., Mirme, S., Hõrrak, U., Berndt, T., Stratmann, F., Birmili, W., Wiedensohler, A., Metzger, A., Dommen, J., Baltensperger, U., Kiendler-Scharr, A., Mentel, T. F., Wildt, J., Winkler, P. M., Wagner, P. E., Petzold, A., Minikin, A., Plass-Dülmer, C., Pöschl, U., Laaksonen, A., and Kulmala, M.: Atmospheric nucleation: highlights of the EUCAARI project and future directions, Atmos. Chem. Phys., 10, 10829–10848, doi:10.5194/acp-10-10829-2010, 2010.
Khosrawi, F. and Konopka, P.: Enhanced particle formation and growth due to mixing processes in the tropopause region, Atmos. Environ., 37(7), 903–910, 2003.
Konopka, P., Günther, G., Müller, R., dos Santos, F. H. S., Schiller, C., Ravegnani, F., Ulanovsky, A., Schlager, H., Volk, C. M., Viciani, S., Pan, L. L., McKenna, D.-S., and Riese, M.: Contribution of mixing to upward transport across the tropical tropopause layer (TTL), Atmos. Chem. Phys., 7, 3285–3308, doi:10.5194/acp-7-3285-2007, 2007.
Krejci, R., Ström, J., de Reus, M., Hoor, P., Williams, J., Fischer, H., and Hansson, H. C.: Evolution of aerosol properties over the rain forest in Surinam, South America, observed from aircraft during the LBA-CLAIRE 98 experiment, J. Geophys. Res.-Atmos., 108(D18), 4561, doi:10.1029/2001JD001375, 2003.
Kulmala, M., Reissell, A., Sipilä, M., Bonn, B., Ruuskanen, T. M., Lehtinen, K. E. J., Kerminen, V.-M., and Ström, J.: Deep convective clouds as aerosol production engines: Role of insoluble organics, J. Geophys. Res., 111, D17202, doi:10.1029/2005JD006963, 2006.
Law, K. S., Fierli, F., Cairo, F., Schlager, H., Borrmann, S., Streibel, M., Real, E., Kunkel, D., Schiller, C., Ravegnani, F., Ulanovsky, A., D'Amato, F., Viciani, S., and Volk, C. M.: Air

ACPD
11, 9249–9312, 2011

mass origins influencing TTL chemical composition over West Africa during 2006 summer monsoon, Atmos. Chem. Phys., 10, 10753–10770, doi:10.5194/acp-10-10753-2010, 2010.
Lee, S. H., Reeves, J. M. , Wilson, J. C. , Hunton, D. E., Viggiano, A. A., Miller, T. M., Ballenthin, J. O., and Lait, L. R.: Particle formation by ion nucleation in the upper troposphere and lower stratosphere, Science, 301(5641), 1886–1889, 2003.
Lee, S. H., Wilson, J. C., Baumgardner, D., Herman, R. L., Weinstock, E. M., LaFleur, B. G., Kok, G., Anderson, B., Lawson, P., Baker, B., Strawa, A., Pittman, J. V., Reeves, J. M., and Bui, T. P.: New particle formation observed in the tropical/subtropical cirrus clouds, J. Geophys. Res.-Atmos., 109(D20), D20209, doi:20210.21029/22004JD005033, 2004.
Lelieveld, J., Crutzen, P. J., Ramanathan, V., Andreae, M. O., Brenninkmeijer, C. A. M., Campos, T., Cass, G. R., Dickerson, R. R., Fischer, H., de Gouw, J. A., Hansel, A., Jefferson, A., Kley, D., de Laat, A. T. J., Lal, S., Lawrence, M. G., Lobert, J. M., Mayol-Bracero, O. L., Mitra, A. P., Novakov, T., Oltmans, S. J., Prather, K. A., Reiner, T., Rodhe, H., Scheeren, H. A., Sikka, D., and Williams, J.: The Indian Ocean Experiment: Widespread Air Pollution from South and Southeast Asia, Science, 291, 1031–1036, 2001.
Li, K.-F., Cageao, R. P., Karpilovsky, E. M., Mills, F. P., Yung, Y. L., Margolis, J. S., and Sander, S. P.: OH column abundance over Table Mountain Facility, California: AM-PM diurnal asymmetry, Geophys. Res. Lett., 32, L13813, doi:10.1029/2005GL022521, 2005.
Lovejoy, E. R., Curtius, J., and Froyd, K. D.: Atmospheric ion-induced nucleation of sulfuric acid and water, J. Geophys. Res.-Atmos., 109(D8), D08204, doi:08210.01029/02003JD004460, 2004.
Lovejoy, E. R. and Curtius, J.: Cluster Ion Thermal Decomposition (II): Master Equation Modeling in the Low-Pressure Limit and Fall-Off Regions. Bond Energies for HSO_4-$(H_2SO_4)x(HNO_3)y$, J. Phys. Chem. A, 105, 10874–10883, 2001.
Lucas, D. D. and Akimoto, H.: Evaluating aerosol nucleation parameterizations in a global atmospheric model, Geophys. Res. Lett., 33 L10808, doi:10810.11029/12006GL025672, 2006.
Merikanto, J., Napari, I., Vehkamäki, H., Anttila, T., and Kulmala, M.: New parameterization of sulfuric acid-ammonia-water ternary nucleation rates at tropospheric conditions, J. Geophys. Res.-Atmos., 112(D15), D15207, doi:10.1029/2006JD007977, 2007.
Metzger, A., Verheggen, B., Dommen, J., Duplissy, J., Prevot, A. S. H., Weingartner, E., Riipinen, I., Kulmala, M., Spracklen, D. V., Carslaw, K. S., and Baltensperger, U.: Evidence for the role of organics in aerosol particle formation under atmospheric conditions, P. Natl. Acad. Sci. USA , 107(15), 6646–6651, doi:10.1073/pnas.0911330107, 2010.

ACPD
11, 9249–9312, 2011

Minikin, A., Petzold, A., Ström, J., Krejci, R., Seifert,M., van Velthoven, P., Schlager, H., and Schumann, U.: Aircraft observations of the upper tropospheric fine particle aerosol in the Northern and Southern Hemispheres at midlatitudes, Geophys. Res. Lett., 30(10), 1503, doi:1510.1029/2002GL016458, 2003.

Mirme, S., Mirme, A., Minikin, A., Petzold, A., Hõrrak, U., Kerminen, V.-M., and Kulmala, M.: Atmospheric sub-3 nm particles at high altitudes, Atmos. Chem. Phys., 10, 437–451, doi:10.5194/acp-10-437-2010, 2010.

Murphy, D. M., Thomson, D. S., and Mahoney, M. J.: In situ measurements of organics, meteoritic material, mercury, and other elements in aerosols at 5 to 19 kilometers, Science, 282(5394), 1664–1669, 1998.

Murphy, D. M., Cziczo, D. J., Froyd, K. D., Hudson, P. K., Matthew, B. M., Middlebrook, A. M., Peltier, R. E., Sullivan, A., Thomson, D. S., and Weber, R. J.: Single-particle mass spectrometry of tropospheric aerosol particles, J. Geophys. Res., 111, D23S32, doi:10.1029/2006JD007340, 2006.

O'Brien, K.: The theory of cosmic-ray and high-energy solar-particle transport in the atmosphere, in: The natural radiation environment VII, edited by: McLaughlin, J. P. and Simopoulos, E. S., and Steinhäusler, F., Proceedings of the Seventh International Symposium on the Natural Radiation Environment, Rhodes, Greece, 20–24 May, 2002, Elsevier, 2005.

Riediger, O., Volk, C. M., Strunk, M., and Schmidt, U.: HAGAR- A new in situ tracer instrument for stratospheric balloons and high altitude aircraft, Eur. Comm. Air Pollut. Res. Report 73, 727–730, 2000.

Schumann, U.: TROCCINOX – Tropical Convection, Cirrus and Nitrogen Oxides Experiment, Overview, General Assembly 2005 of the European Geosciences Union, Vienna, Austria, 24–29 April 2005, 2005.

Schumann, U. and Huntrieser, H.: The global lightning-induced nitrogen oxides source, Atmos. Chem. Phys., 7, 3823–3907, doi:10.5194/acp-7-3823-2007, 2007.

Schiller, C., Grooß, J.-U., Konopka, P., Plöger, F., Silva dos Santos, F. H., and Spelten, N.: Hydration and dehydration at the tropical tropopause, Atmos. Chem. Phys., 9, 9647–9660, doi:10.5194/acp-9-9647-2009, 2009.

Seinfeld, J. H. and Pandis, S. N.: Atmospheric Chemistry and Physics - From Air Pollution to Climate Change (2nd edition), John Wiley & Sons, 2006.

Shur, G. H., Sitnikov, N. M., and Drynkov, A. V.: A mesoscale structure of meteorological ?elds in the tropopause layer and in the lower stratosphere over the Southern tropics (Brazil), Russ.

ACPD
11, 9249–9312, 2011

Meteorol. Hydrol., 32, 48749, 2007.
Sokolov, L. and Lepuchov, B.: Protocol of interaction between Unit for Connection with Scientific Equipment (UCSE) and on-board scientific equipment of Geophysica aircraft (Second edition), Myasishchev Design Bureau (MDB), 1998.
Stohl, A., Wotawa, G., Seibert, P., and Kromp-Kolb, H.: Interpolation errors in wind fields as a function of spatial and temporal resolution and their impact on different types of kinematic trajectories, J. Appl. Meteor., 34, 2149–2165, 1995.
Stohl, A., Hittenberger, M., and Wotawa, G.: Validation of the Lagrangian particle dispersion model FLEXPART against large scale tracer experiments, Atmos. Environ., 32, 4245–4264, 1998.
Stohl, A., Haimberger, L., Scheele, M. P., and Wernli, H.: An intercomparison of results from three trajectory models, Meteor. Appl., 8, 127–135, 2001.
Stohl, A., Forster, C., Eckhardt, S., Spichtinger, N., Huntrieser, H., Heland, J., Schlager, H., Wilhelm, S., Arnold, F., and Cooper, O.: A backward modeling study of intercontinental pollution transport using aircraft measurements, J. Geophys. Res.-Atmos., 108(D12), 4370, doi:10.1029/2002JD002862, 2003.
Stohl, A., Forster, C., Frank, A., Seibert, P., and Wotawa, G.: Technical note: The Lagrangian particle dispersion model FLEXPART version 6.2, Atmos. Chem. Phys., 5, 2461–2474, doi:10.5194/acp-5-2461-2005, 2005.
Stohl, A., Andrews, E., Burkhart, J. F., Forster, C., Herber, A., Hoch, S. W., Kowal, D., Lunder, C. Mefford, T. , Ogren, J. A., Sharma, S., Spichtinger, N., Stebel, K., Stone, R., Ström, J., Tørseth, K., Wehrli, C., and Yttri, K. E.: Pan-Arctic enhancements of light absorbing aerosol concentrations due to North American boreal forest fires during summer 2004, J. Geophys. Res., 111, D22214, doi:10.1029/2006JD007216, 2006.
Thomason, L. and Peter, T. (Eds.): SPARC Assessment of Stratospheric Aerosol Properties, WCRP-124, WMO/TD-No. 1295, SPARC Report No. 4, Toronto, Canada, 2006.
Thornton, D. C., Bandy, A. R., Blomquist, B. W., Bradshaw, J. D., and Blake, D. R.: Vertical transport of sulfur dioxide and dimethyl sulfide in deep convection and its role in new particle formation, J. Geophys. Res., 102(D23), 28501–28509, 1997.
Twohy, C. H., Clement, C. F., Gandrud, B. W., Weinheimer, A. J., Campos, T. L., Baumgardner, D., Brune, W. H., Faloona, I., Sachse, G. W., Vay, S. A., and Tan, D.: Deep convection as a source of new particles in the midlatitude upper troposphere, J. Geophys. Res., 107(D21), 4560, doi:10.1029/2001JD000323, 2002.

ACPD
11, 9249–9312, 2011

Viciani, S., D'Amato, F., Mazzinghi, P., Castagnoli, F., Toci, G., and Werle, P. A.: A cryogenically operated laser diode spectrometer for airborne measurement of stratospheric trace gases, Appl. Phys. B., 90, 581–592, 2008.

Wang, S., Pickett, H. M., Pongetti, T. J., Cheung, R., Yung, Y. L., Shim, C., Li, Q., Canty, T., Salawitch, R. J., Jucks, K. W., Drouin, B., and Sander, S. P.: Validation of Aura Microwave Limb Sounder OH measurements with Fourier Transform Ultra-Violet Spectrometer total OH column measurements at Table Mountain, California, J. Geophys. Res., 113, D22301, doi:10.1029/2008JD009883, 2008.

Weber, R. J., McMurry, P. H., Eisele, F. L., and Tanner, D. J.: Measurement of Expected Nucleation Precursor Species and 3-500-Nm Diameter Particles at Mauna-Loa-Observatory, Hawaii, J. Atmos. Sci., 52(12), 2242–2257, 1995.

Weber, R. J., McMurry, P. H., Mauldin, R. L., Tanner, D. J., Eisele, F. L., Clarke, A. D., and Kapustin, V. N.: New particle formation in the remote troposphere: A comparison of observations at various sites, Geophys. Res. Lett., 26(3), 307–310, 1999.

Weinzierl, B., Petzold, A., Esselborn, M., Wirth, M., Rasp, K., Kandler, K., Schütz, L., Koepke, P., and Fiebig, M.: Airborne measurements of dust layer properties, particle size distribution and mixing state of Saharan dust during SAMUM 2006, Tellus, 61B, 96–117, doi:10.1111/j.1600-0889.2008.00392.x, 2009.

Weigel, R., Hermann, M., Curtius, J., Voigt, C., Walter, S., Böttger, T., Lepukhov, B., Belyaev, G., and Borrmann, S.: Experimental characterization of the COndensation PArticle counting System for high altitude aircraft-borne application, Atmos. Meas. Tech., 2, 243–258, doi:10.5194/amt-2-243-2009, 2009.

Wilson, J. C., Jonsson, H. H., Brock, C. A., Toohey, D. W., Avalone, L. M., Baumgardner, D., Dye, J. E., Poole, L. R., Woods, D. C., DeCoursey, R. J., Osborne, M., Pitts, M. C., Kelly, K. K., Chan, K. R., Ferry, G. V., Loewenstein, M., Podolske, J. R., and Weaver, S.: In situ observations of aerosol and chlorine monoxide after the 1991 eruption of Mount Pinatubo: effect of reactions on sulfate aerosol, Science, 261, 1140–1143, 1993.

Wilson, J. C., Lee, S.-H., Reeves, J. M., Brock, C. A., Jonsson, H. H., Lafleur, B. G., Loewenstein, M., Podolske, J., Atlas, E., Boering, K., Toon, G., Fahey, D., Bui, T. P., Diskin, G., and Moore, F.: Steady-state aerosol distributions in the extra-tropical, lower stratosphere and the processes that maintain them, Atmos. Chem. Phys., 8, 6617–6626, doi:10.5194/acp-8-6617-2008, 2008.

Yu, F. Q. and Turco, R. P.: From molecular clusters to nanoparticles: Role of ambient ionization

ACPD
11, 9249–9312, 2011

in tropospheric aerosol formation, J. Geophys. Res.-Atmos., 106(D5), 4797–4814, 2001.
Zhang, R. Y., Suh, I. Zhao, J., Zhang, D., Fortner, E. C., Tie, X., Molina, L. T., and Molina, M. J.: Atmospheric new particle formation enhanced by organic acids, Science, 304(5676), 1487–1490, 2004.

ACPD
11, 9249–9312, 2011

Table 1. Occurrence frequency of 68 single NPF events observed aboard the M-55 "Geophysica" and of 266 single NPF events observed aboard the DLR-Falcon as a function of potential temperature (in 10 K bins, for $\Theta > 340$ K). The number concentration N_{uf} is given as the arithmetic mean together with the maximum and minimum value of N_{uf} reached in respective $\Theta-$ bin. The NPF duration is given as a range between shortest and longest duration of an event with a total NPF duration for respective $\Theta-$ bin. The total measurement time reflects the residence time of the two aircraft in each $\Theta-$ bin throughout the TROCCINOX and SCOUT-AMMA mission. Note a mean aircraft ground speed of $\sim$170($\pm$80) m s^{-1} (M-55 "Geophysica") and $\sim$200($\pm$20) m s^{-1} (DLR – Falcon 20).

	Θ range in K	number of NPF events	concentration in cm^{-3} $\overline{N_{uf}}$	N_{uf}^{min}	N_{uf}^{max}	NPF duration range in s	total NPF duration in s	total measurement time in s
M-55 "Geophysica"	430–440	1	11	11	11	15	15	2910
	420–429	1	15	15	15	120	120	8250
	410–419	2	110	63	228	390–1710	2100	22 425
	390–399	4	28	12	43	15–90	135	33 975
	380–389	1	64	33	423	15–705	1845	22 590
	370–379	13	205	23	1164	15–1935	3795	24 435
	360–369	18	825	24	6777	15–1290	6150	28 005
	350–359	16	2114	81	16517	15–2610	6930	24 900
DLR-Falcon 20	340–349	191	392	100	4812	20–1500	25 620	111 550
	330–339	25	271	100	2881	20–310	1570	19 450
	320–329	7	373	123	1022	20–230	440	12 100
	310–319	6	458	106	1548	20–50	200	14 250
	300–309	26	2644	106	23 572	20–420	1370	9390
	290–299	5	587	119	2380	20–100	250	740

ACPD
11, 9249–9312, 2011

Table 2. Input parameters for MAIA model runs for calculations of the ion-induced and neutral aerosol nucleation for the case studies displayed in Fig. 6. Values of temperature (T), pressure (p) and relative humidity with respect to water (RHw) are given at the time the NPF is initialized after convective uplift. Water vapor and OH are given in number of molecules per cm^3 of air.

		initial conditions at trajectory start					
trajectories end date and time (UTC)	Fig. 6 panel	T in K	p in hPa	RHw in %	H_2O vapor in cm^{-3}	noon OH in cm^{-3}	ion pair production rate in $cm^{-3}s^{-1}$
24 Feb 2005, 14:13:17	(a)	227	295	62	6.1×10^{15}	10^6	18.1
24 Feb 2005, 14:16:34	(b)	227	171	41	2.7×10^{14}	10^6	23.8
7 Aug 2006, 14:09:30	(c)	227	240	48	2.4×10^{15}	10^6	24.1
7 Aug 2006, 15:36:44	(d)	227	161	59	1.9×10^{15}	10^6	21.1

ACPD
11, 9249–9312, 2011

Table 3. Ice cloud microphysical parameters for the cloud events during NPF observation measured on board the M-55 "Geophysica" by the FSSP-100 and the CIP as well as the cloud particle volume backscatter coefficient and depolarization measured by the MAS instrument (SCOUT-AMMA). Note that the last column refers to the cloud parameters when ultrafine particles fully disappear.

	South America	West Africa			
	NPF Case 1	NPF Case 2, Ice-cloud I	NPF Case 3, Ice-cloud II	NPF Case 3, Ice-cloud III	N_{uf} = 0 Ice-cloud III
averaging time in s	262	98	83	20	2
covered flight distance in km	35.3	12.7	11.8	2.8	0.2
altitude in km	13	12.2	12.6	12.5	11.9
potential temperature in K	351	349	350	348	350
N_{uf} in cm^{-3}	260–7700	650–4000	<1300	<750	≈0
ice cloud particle properties					
averaged number concentration in cm^{-3}	0.1	0.4	0.3	0.3	4.4
surface area in μm^2 cm^{-3} for d_p range in µm	52.2 2.7-29.7	3.5×10^6 2.7–1600	7.9×10^5 2.7–1600	3.4×10^6 2.7–1600	2.6×10^7 2.7–1600
averaged aerosol volume backscatter coeff. in m^{-1} sr^{-1}	–	$(1.6\pm1) \times 10^6$	$(1.6\pm1) \times 10^6$	$(3.8\pm3) \times 10^6$	12×10^6
averaged aerosol volume depolarization in %	–	62 ± 6	58 ± 4	59 ± 5	78

ACPD
11, 9249–9312, 2011

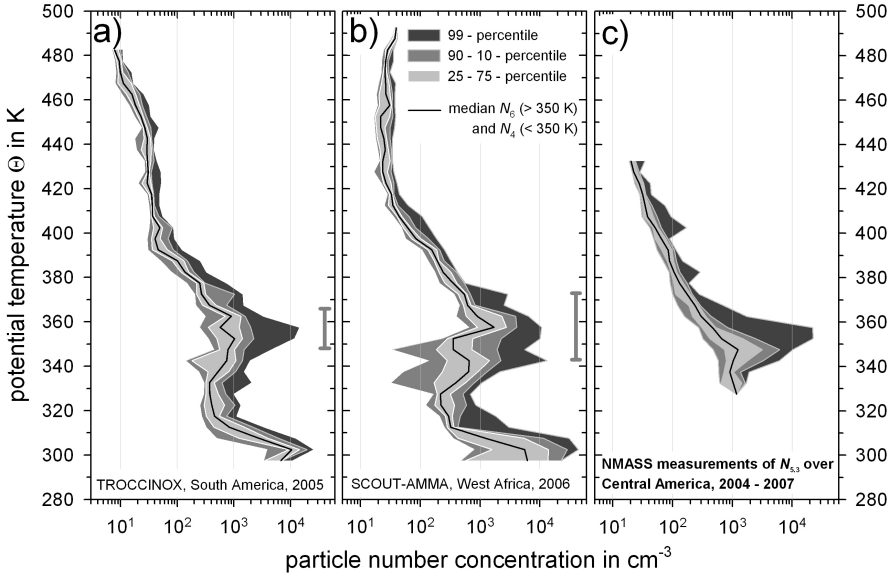

Fig. 1. Vertical profiles of total particle number densities (for size diameters larger than 6 and 4 nm up to ≈1 µm) for all tropical flights of the M-55 "Geophysica" and the DLR Falcon-20 during **(a)** TROCCINOX and **(b)** SCOUT-AMMA. Median values are shown (black line), as well as 10-, 25-, 75-, 90-, and 99-percentiles (grey-scale contours). The frequent occurrence of New Particle Formation events influences the total number concentration at South America particularly in the 11–13.5 km altitude range or rather in the 9–14 km altitude range at West Africa. These altitude bands are displayed in both figure panels by a vertical bar. **(c)** Measurement results from the NMASS on board the NASA WB-57F over Central America in the tropics (red circles) measured over 4 yr (between 2004 and 2007) show the frequent occurrence of high particle number densities (for size diameters >5.3 nm) coincidently in this altitude band.

ACPD
11, 9249–9312, 2011

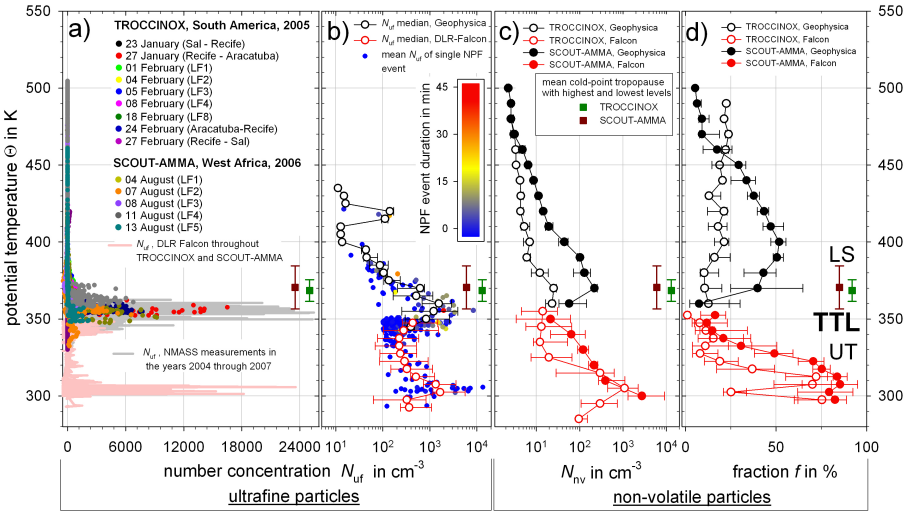

Fig. 2. **(a)** Concentrations of ultrafine particles, N_{uf}, in the size range between 6 nm < d_p < 15 nm as measured by COPAS during 9 tropical flights of the M-55 "Geophysica" from TROCCINOX (4 transfer and 5 local flights) and from 5 local flights within SCOUT-AMMA. The resulting median vertical distribution of N_{uf} is shown as black scatter-line plot with 25- and 75-percentiles. Additionally, N_{uf} (5.3 nm < d_p < 15 nm) resulting from 4 yr of measurements on board the NASA WB-57F with the NMASS (grey shaded) are displayed. Above 380 K no significant concentrations of nucleation mode particles were observed. Below 380 K high densities of ultrafine particles indicate recent new particle formation. **(b)** Median vertical profile with 25- and 75-percentiles of the number concentration of non-volatile particles (N_{nv}) with d_p > 10 nm and **(c)** Median vertical profile with 25- and 75-percentiles of the fraction f (=N_{nv}/N_6) of non-volatile particles. M-55 "Geophysica" measurements are denoted as filled circles and the DLR Falcon-20 data as open circles. The squares mark the mean cold point tropopause in green for TROCCINOX and in dark-red for SCOUT-AMMA with the vertical bars denoting the highest and lowest encountered tropopause heights.

ACPD
11, 9249–9312, 2011

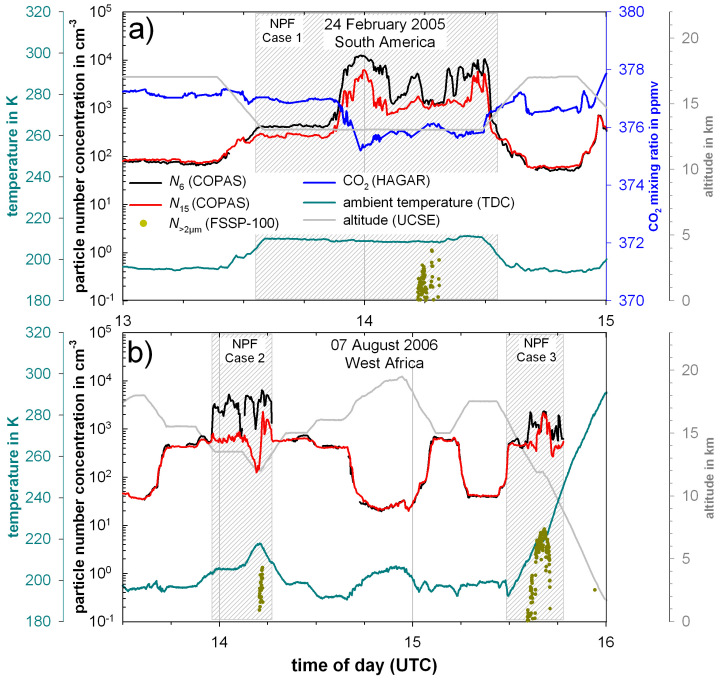

Fig. 3. Cases of increased densities of ultrafine particles indicating New Particle Formation (NPF – shaded areas): **(a)** Case 1 during the flight from Araçatuba to Recife, Brazil, on 24 February 2005 (TROCCINOX) and **(b)** Cases 2 and 3 during a local flight over West Africa on 7 August 2006 (SCOUT-AMMA). The difference in N_6 (black) and N_{15} (red) particle concentrations is indicative of recent NPF. The flight altitudes are shown in grey, ambient temperatures in dark-cyan, and in situ measured CO_2 mixing ratio in blue (upper panel). CO_2 data are not available for the SCOUT-AMMA flight on 7 August 2006. The flight time period inside a cirrus cloud is indicated by $N_{>2\,\mu m}$ as detected by FSSP-100 measurements (green dots). Note that the gaps in the N_6 time series of panel **(b)** are caused by discarding data in case the measurements were affected by electronic noise.

ACPD
11, 9249–9312, 2011

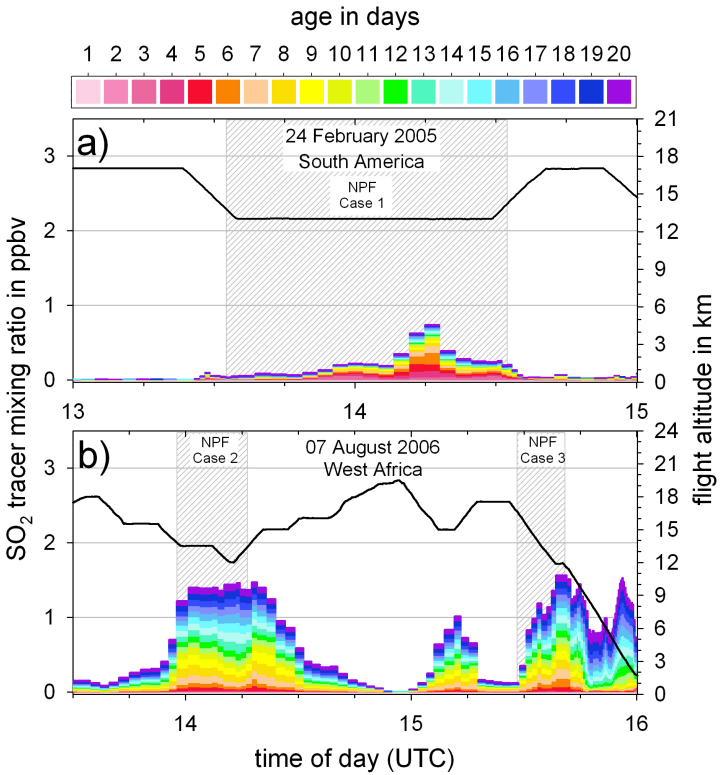

Fig. 4. FLEXPART model simulation of SO_2 mixing ratio along the flight track. The FLEXPART model predicts high SO_2 values exactly for those parts of the flight, where the strongest nucleation (i.e., the highest concentrations of ultrafine particles denoted as NPF Case 1, 2, 3) was observed. The FLEXPART model does not consider any processing of SO_2 during atmospheric transport and the given values are upper limits only. (See text for detailed explanation of colors and scales.)

ACPD
11, 9249–9312, 2011

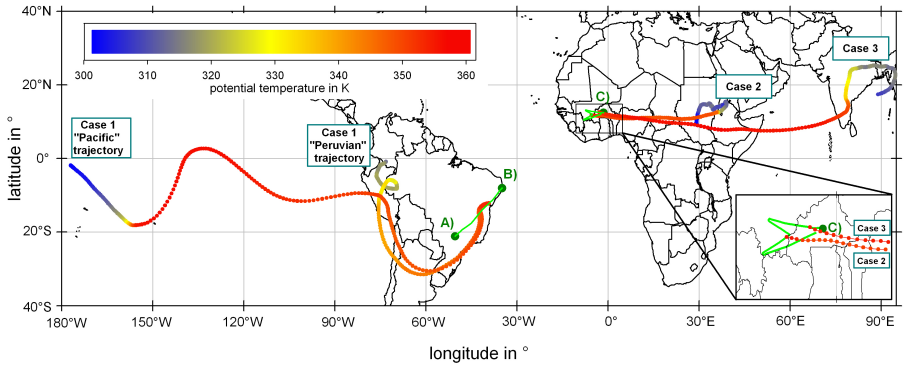

Fig. 5. Air mass trajectory pathways for the NPF cases from different source regions intersecting the M-55 Geophysica flight tracks (green) between **(A)** Araçatuba and **(B)** Recife, Brazil (Case 1, TROCCINOX) or during a local flight with departure and destination at **(C)** Ouagadougou, Burkina Faso (Case 2 and 3, SCOUT-AMMA), determined from FLEXTRA simulations and on which the MAIA runs are based. Trajectories are colored according to the potential temperature evolution along their pathways indicating vertical air mass movement. A close-up (bottom right) serves to illustrate where in detail the trajectories intersect with the SCOUT-AMMA flight track on 7 August 2006.

ACPD
11, 9249–9312, 2011

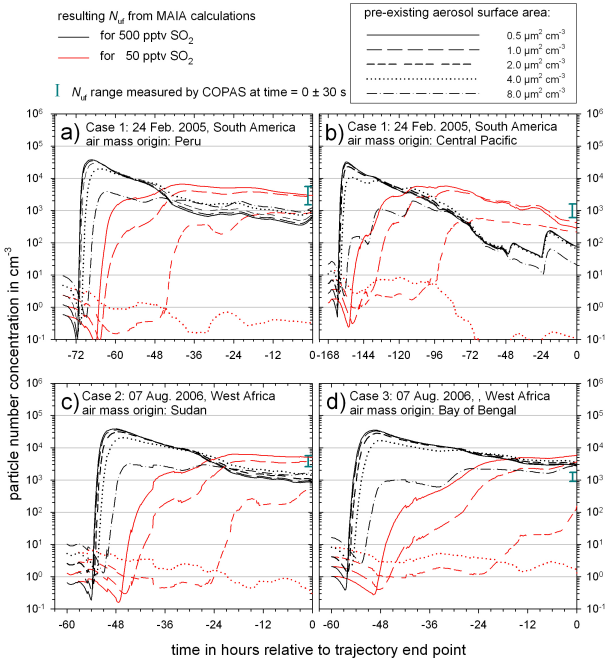

Fig. 6. Model calculation of N_{uf} as measure for the strength of NPF caused by neutral and ion-induced aerosol nucleation from calculations by the kinetic aerosol model MAIA. See text and Table 2 for details and model input parameters. Each panel shows the number of particles produced by neutral and ion-induced nucleation of binary solution of H_2SO_4, oxidized from pre-existing SO_2, and H_2O as function of time before the air parcel was sampled by the aircraft at time = 0 and as a function of pre-existing aerosol surface area. Black lines show the result considering a pre-existing SO_2 mixing ratio of 500 pptv while the red lines represent the calculation results based on 50 pptv initial SO_2 mixing ratio. The cyan circles in each panel indicate the particle number concentration N_{uf} measured by COPAS at time = 0 (slightly displaced from time = 0 for clearer illustration) according to respective trajectory crossing with the Geophysica flight path.

ACPD
11, 9249–9312, 2011

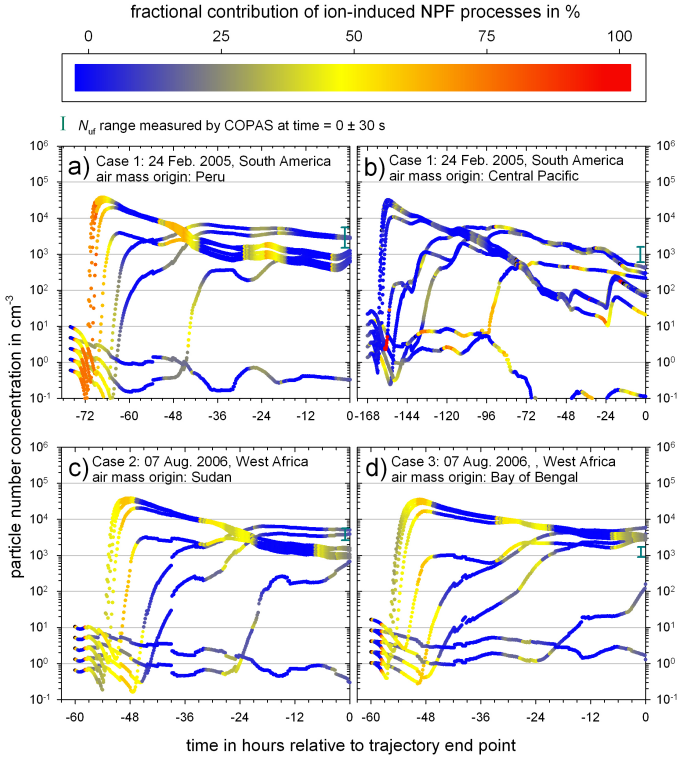

Fig. 7. As Fig. 6 with the different runs of MAIA calculations colored according to the respective fractional contribution of the ion-induced NPF process.

ACPD
11, 9249–9312, 2011

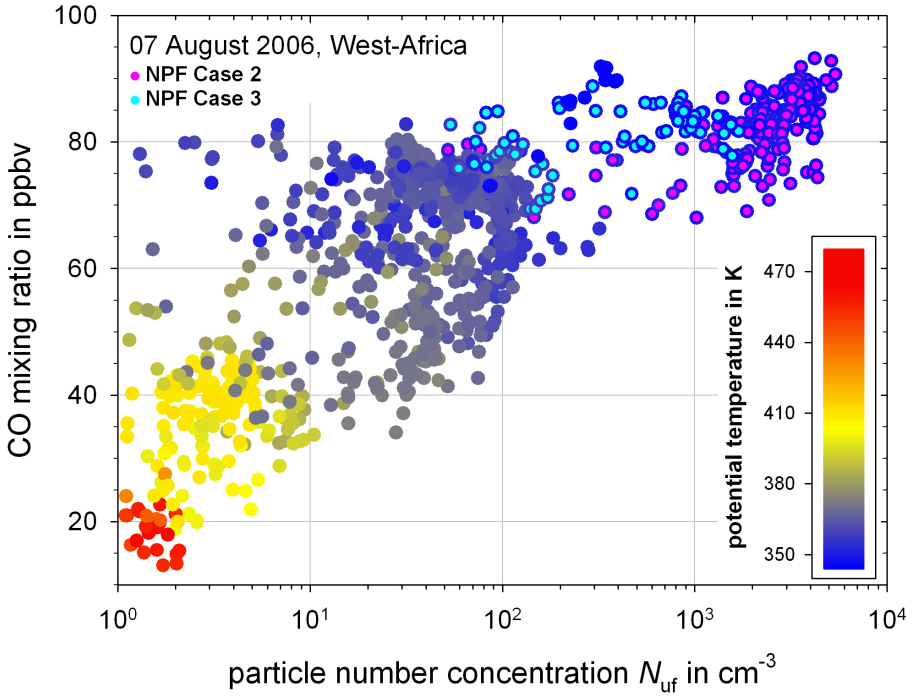

Fig. 8. Carbon monoxide (CO) mixing ratio (from the COLD instrument) versus particle number concentration N_{uf} measured by COPAS during a flight on 7 August 2006 (SCOUT-AMMA). The data points are colored according to the potential temperature. Values of N_{uf} smaller than 1 have been discarded from consideration for this figure. The COPAS samples of NPF Case 2 (pink) and NPF Case 3 (cyan) are highlighted. The maximum CO mixing ratios were suggested to originate from anthropogenic emissions in Asia (for details see text or Law et al., 2010).

ACPD
11, 9249–9312, 2011

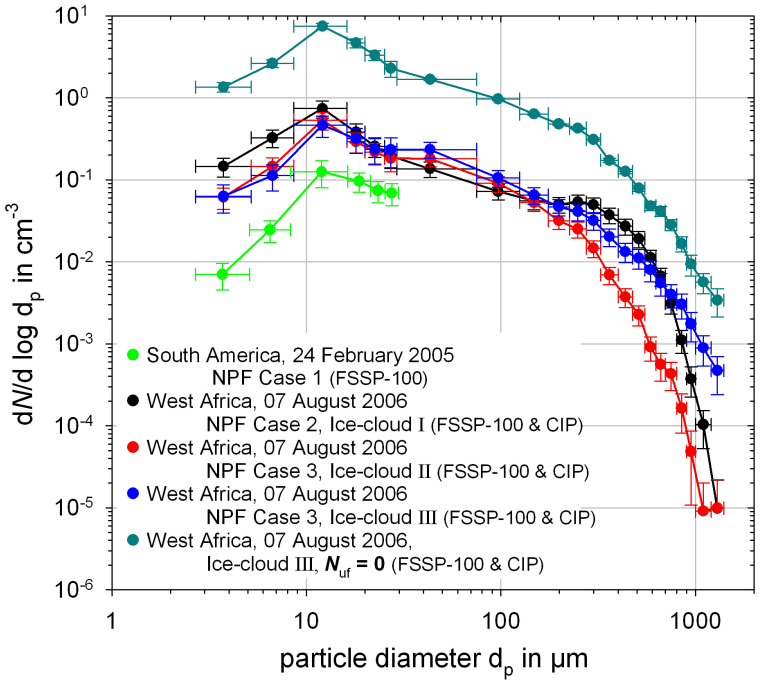

Fig. 9. Cloud particle size distributions in terms of particle size diameter, d_p, as measured by the FSSP-100 (24 February 2005), and the combination of FSSP-100 with Cloud Imaging Probe (CIP, 7 August 2006). The vertical error bars denote uncertainties for the size of the sample volumes and due to counting statistics, horizontal error bars illustrate the particle size bin width. The encounter of Case 1 was an upper tropospheric cirrus cloud while Case 3 was the anvil of a West African monsoon Mesoscale Convective System (MCS). Case 2 cirrus cloud was found to be related to recent convection, but no indication clearly relates Case 2 to MCS outflow.

ACPD
11, 9249–9312, 2011

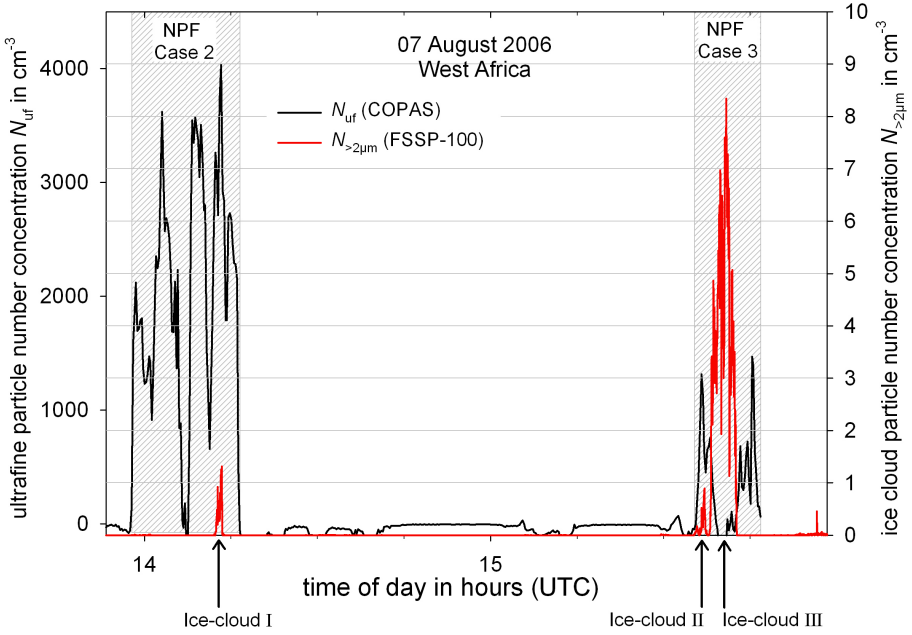

Fig. 10. Close-up of the time series of measured number concentration of ultrafine particles N_{uf} (COPAS, black line) and of ice cloud particles $N_{>2\,\mu m}$ (FSSP-100, red line) of the M-55 "Geophysica" flight on 7 August 2006 over West Africa. This is an illustration for the observation of ultrafine particles in concentrations of 170–1000 cm^{-3} in presence of ice cloud particles (1.3–0.9 cm^{-3}, ice cloud I and II). For increased ice particle concentrations (>2 cm^{-3}) the newly formed ultrafine particles nearly fully disappear (Ice-cloud III).

ACPD
11, 9249–9312, 2011